*Earth and Environmental Science Transactions of the Royal Society of Edinburgh,* **99**, 225–250, 2009 (for 2008)

# A reactive assimilation model for regional-scale cordierite-bearing granitoids: geochemical evidence from the Late Variscan granites of the Central Iberian Zone, Spain

J. M. Ugidos[1], W. E. Stephens[2], A. Carnicero[1] and R. M. Ellam[3]

[1] Departamento de Geología, Facultad de Ciencias, 37008 Salamanca, Spain
Email: jugidos@usal.es

[2] School of Geography & Geosciences, University of St Andrews, St Andrews, Fife, KY16 9AL, Scotland, UK

[3] Scottish Universities Environmental Research Centre, East Kilbride G75 OQF, Scotland, UK

ABSTRACT: Regional scale biotite and cordierite-bearing granites (*s.l.*) in the Variscan of the Central Iberian Zone (CIZ) are spatially closely associated with cordierite-rich nebulites and cordierite-bearing two-mica granites, and with cordierite-rich high grade hornfelses and cordieritites (>60% cordierite) that are relatively common in the aureoles of these granites. Building on published field evidence, petrological data are presented which, combined with new chemical and isotopic (Sr–Nd) modelling, indicate that the cordierite-bearing granites cannot be derived by simple anatexis of regional sedimentary protoliths; but the data are consistent with a process of reactive assimilation that involves the interaction of biotite granite magma with high-grade host rocks ranging from cordierite nebulites to andalusite-bearing cordieritites. The contribution of the postulated cordierite-rich contaminants to the diversity of cordierite granite compositions is modelled using the compositions of regional Lower Cambrian–Upper Neoproterozoic metasedimentary rocks that are generally chemically mature (CaO very rarely exceeds 1·4%). These rocks include specific horizons in which extreme chemical alteration is attributable to sediment reworking during eustatic falls in sea level. Such compositions may account for the presence of the high concentrations in Al that later produced cordieritites. Fractional crystallisation is also important, particularly in generating the more evolved cordierite granite and cordierite biotite muscovite granite compositions. Although assimilation *in situ* is normally regarded as a minor contributor volumetrically to evolving plutons, in this instance the emplacement of large volumes of granite magma into a high-T–low-P environment significantly increased the potential for reactive assimilation.

KEY WORDS: anatexis, Central Iberia, cordierite granite, nebulite

Assimilation is capable of modifying bulk magma compositions in the very deep crust (Hildreth & Moorbath 1988), especially during fractional crystallisation (Bowen 1928; DePaolo 1981). There is more scepticism about the ability of silicic magmas to assimilate country rocks at high levels in the crust. The objections are two-fold. First it is argued that thermal budgets are inadequate to bring about large-scale bulk melting, especially when the assimilating magma is granitic (Spera & Bohrson 2001). Secondly bulk assimilation is often difficult to establish on the basis of field, petrographic and geochemical evidence. However, the process of reactive bulk assimilation significantly reduces the additional thermal energy requirements (Beard *et al.* 2005) and makes assimilation an effective processes in the continental crust. New petrographic and geochemical evidence such as the detection of inherited minerals (notably zircons) and heterogeneous isotope systems at the grain level are lending support to a greater role for open system processes (Knesel *et al.* 1999). The aim of this study is to compare the evidence for bulk assimilation with that for anatexis in the petrogenesis of regional-scale cordierite granites among the Variscan high-T–low-P metamorphic zones of central Spain.

Cordierite granites have special significance in petrogenesis (the term granite is used *sensu lato* throughout to include granodiorites and monzonites), cordierite in a felsic matrix being taken to indicate crystallisation from, or equilibration with a strongly peraluminous magma derived typically from melting a metasedimentary source. In the cordierite granites and associated volcanics of the Lachlan fold belt of SE Australia, it has been argued that diversity relates to differential segregation or separation of restite (Chappell & White 2001). However, fractional crystallisation, magma mixing and wall-rock contamination are all capable of modifying more metaluminous precursor magmas to generate peraluminous mineral assemblages in large volumes (Patiño-Douce 1999). The origin of cordierite in granites is also controversial, being potentially magmatic, xenocrystic, restitic, or metasomatic (Clarke 1995).

Understanding the origin of regional-scale cordierite granites is important particularly in collisional orogens (Pitcher 1997), where they may be associated with major mineral deposits. Such granites are particularly common in the high-T–low-P metamorphic belts of the Variscan of Europe. In contrast to their metaluminous equivalents in cordilleran belts

 doi:10.1017/S1755691009008159

and post-collisional orogens, cordierite granite plutons have received relatively little attention. This paper examines an extensive region of cordierite granites in the Central Iberian Zone (CIZ), where there is an intimate relationship between migmatites, cordierite granites and metaluminous granites.

Peraluminous magmas may result from a relatively wide range of processes that may or may not involve pure sedimentary protoliths (Halliday *et al.* 1981; Miller 1985), although those involving fluid-absent melting reactions are considered to be the most common. Experimental studies addressing pelites and greywackes as possible sources for primary melts support the notion that fluid-absent melting reactions only generate peraluminous leucogranites accompanied by residual phases such as cordierite and garnet, and do not generate Mg–Fe-rich granitoid melts (Patiño-Douce & Johnston 1991; Montel & Vielzeuf 1997; Stevens *et al.* 1997). Moreover, at low P (<5 kbar) the melt proportion increases sharply over a limited range of temperature and decreases with increasing pressure at a given temperature (Clemens & Vielzeuf 1987; Montel & Vielzeuf 1997).

With regard to protoliths and major residual phases, it is known that, amongst other factors such a volatile content, a low bulk magnesium number [Mg#=molar $100 \times MgO/(MgO+FeO)$] favours lower solidus temperatures. The abundance of residual cordierite increases at low P and T, whereas the presence of garnet is favoured by increasing pressure and/or decreasing Mg# (Zen 1988). Where cordierite is a major product, the melt fraction is markedly restricted because this mineral is a sink for $H_2O$ (Stevens *et al.* 1997). When biotite breakdown reactions involve sillimanite, the temperature of the pelite solidus is lowered and the production of more cordierite instead of garnet is favoured (Montel & Vielzeuf 1997; Stevens *et al.* 1997).

Cordierite, among other Al-rich minerals, is common in many monzogranite to granodiorite bodies, with Fe, Mg and Ca abundances much higher than those of anatectic leucogranites. Accounting for relatively mafic peraluminous granitoids in the absence of experimental evidence for mafic peraluminous melts may require the involvement of complex processes involving interactions between magmas, assimilation, etc. (Montel & Vielzeuf 1997; Saito *et al.* 2007), rather than from pure melts of sedimentary protoliths. Application of experimental petrology to the origin of Iberian granitoids (e.g. Castro *et al.* 1999, 2000) includes specific investigation of the role of assimilation in cordierite granites (García Moreno *et al.* 2007). Two distinct models are commonly applicable to account for the presence of cordierite in non-anatectic granite magmas (Clarke 1995): (i) those involving the magmatic precipitation of cordierite; and (ii) those favouring a restitic or xenocrystic origin for cordierite and/or the assimilation of cordierite-rich rocks. The former group requires Al enrichment in the melt phase due to Al dissolution from host rocks and/or Al enrichment during magma evolution, whereas the latter group involves a melting process that generates residual cordierite or a more-or-less homogeneous mix of granite magma and cordierite-rich host rocks. These models are not mutually incompatible and the same granite may entrain more than one genetic type of cordierite crystal, although the common presence of extensive pinitisation can make it difficult to resolve the origin of the cordierite solely on the basis of petrographic and chemical data.

An assimilation model consistent with most major oxide and trace element variations (including the rare earth elements (REE)) was proposed for the cordierite granites of the CIZ, but the model did not successfully account for all geochemical observations (Ugidos & Recio 1993). In particular, the relatively high $P_2O_5$ content in these rocks remained unexplained. The assimilation model is revised in the light of a large body of recent experimental petrological studies on the anatexis of metasedimentary materials. Recent studies of the regional geology in Central Spain, both metasedimentary series and granites, have also contributed large datasets of geochemical analyses, including major and trace elements and Sr–Nd isotopes that provide additional constraints for modelling the origin of these granites in the context of the anatexis-assimilation debate. Of particular value is the use of sequence stratigraphy to constrain the characteristics of country rock assimilants. Reactive assimilation is the preferred model for the generation of regional-scale intrusive cordierite-bearing granites at the particular metamorphic conditions of the study region, and it is postulated that it may have wider applicability, as used recently for example, to account for the cordierite tonalites in the margins of the Tokuwa pluton in Japan (Saito *et al.* 2007).

## 1. Geological setting

The cordierite granites of this study are located in the CIZ (Fig. 1) where Upper Neoproterozoic and Lower Cambrian sedimentary series consist mainly of shales and sandstones. Intrusive granites are common, and the largest bodies (hundreds to thousands km$^2$, extending over about 10 000 km$^2$ in Central Spain) are of late Variscan age and range from amphibole-bearing biotite granites to two-mica cordierite-bearing types. Early Variscan autochthonous to sub-autochthonous leucogranites and two-mica granites outcrop in smaller bodies (tens to hundreds km$^2$) in the same region.

The compositions of the country rocks are central to the petrological model developed in the present study, and the application of sequence stratigraphy is useful in demonstrating the regional persistence of unusual compositions that may be responsible for generating enriched compositions in contaminated rocks. The sedimentary succession consists of twelve lithostratigraphic units (Table 1). The detrital lower units I–IV and VI–XII are of Upper Neoproterozoic and Lower Cambrian ages respectively, whereas unit V corresponds to carbonate beds. The whole sequence ranges from 1800 metres to 3900 metres in thickness. The most conspicuous characteristics of these siliciclastic rocks are their petrological and geochemical homogeneity, together with their chemical maturity over an extensive region of more than 30,000 km$^2$ in western Spain. Furthermore, some chemical concentrations such as $TiO_2$ and Zr, together with some elemental ratios (e.g., Rb/Zr<0·65, Ti/Nb>400) and relatively high $\varepsilon_{Nd}$ values in the sequences of the Upper Neoproterozoic ($\varepsilon_{Nd} > -4$), are clearly distinct from those of the Lower Cambrian (Rb/Zr>0·7, Ti/Nb<400, $\varepsilon_{Nd} < -4$), reflecting different sources for the siliciclastic materials of both sequences (Ugidos *et al.* 1997a, b, 2003; Valladares *et al.* 1998, 2000).

Sequence stratigraphy indicates successions formed during falling sea level events. The Upper Neoproterozoic–Lower Cambrian boundary is an unconformity corresponding to a eustatic fall in sea level (Valladares *et al.* 2000, 2006) that led to the subaerial exposure of the uppermost Neoproterozoic. The consequence was severe chemical alteration of the siliciclastic material, resulting in intense leaching of Ca and Na as well as the redistribution of some trace elements (principally Y and the rare earth elements). These chemical effects are found in detrital rocks underlying, and especially overlying, this regional-scale unconformity, and sequence stratigraphy predicts the presence of other such unconformities, notably at the lower boundary of the Upper Neoproterozoic sequence, with similar extreme compositional characteristics (Ugidos *et al.*

https://doi.org/10.1017/S1755691009008159 Published online by Cambridge University Press

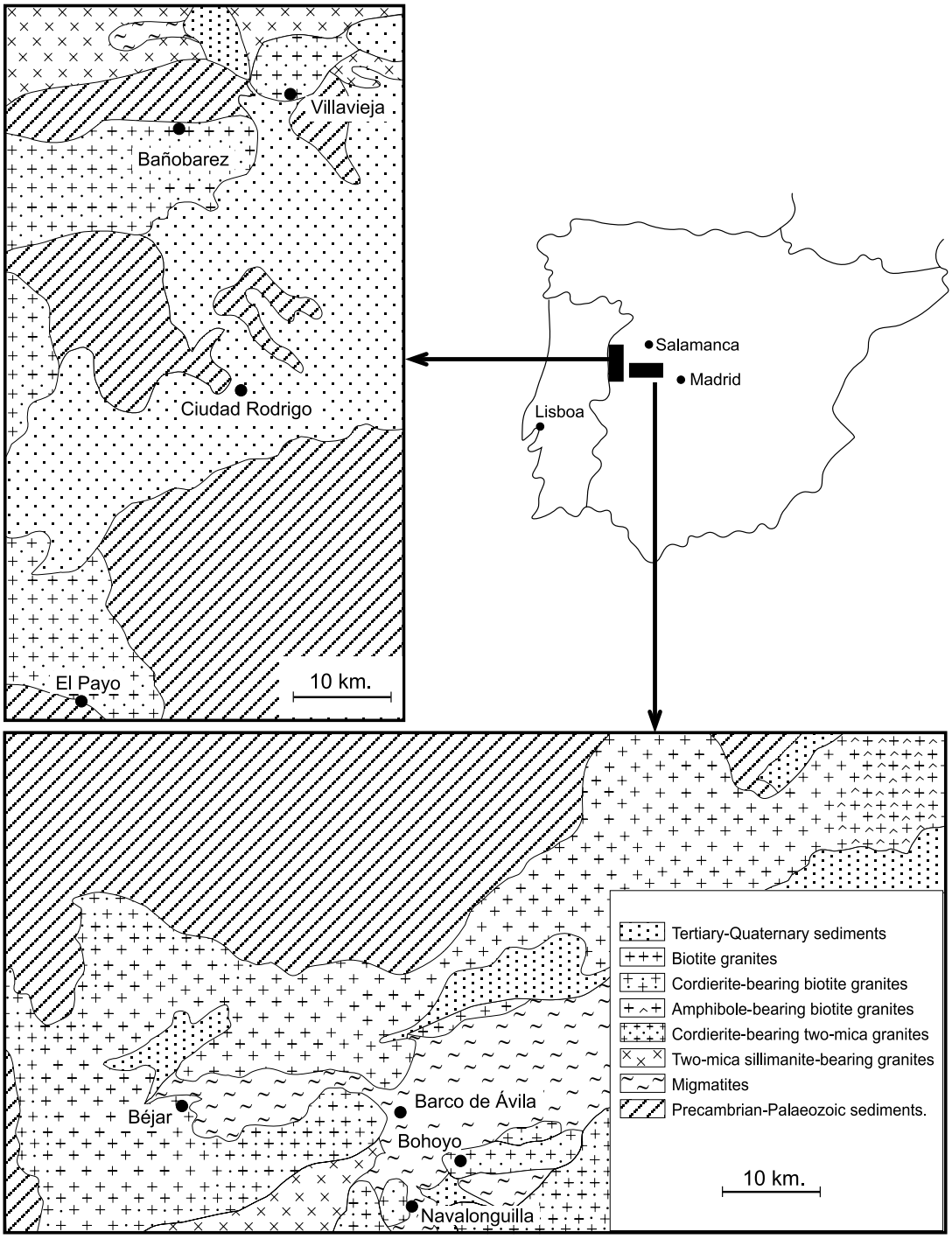


**Figure 1** Geology of the cordierite granite-rich regions S and W of Salamanca. Maps simplified from Carnicero (1983) and Ugidos *et al.* (1988, 1990).

1997a, b, 2003a; Valladares *et al.* 1998, 2000). The important implication for the purposes of this present study is that the sedimentary succession that hosts the granites and was subject to Variscan high T/low P regional metamorphism contains at least one, and probably multiple, horizons that have suffered extreme chemical alteration.

Tectonometamorphic events began with early Variscan intermediate pressure (5–7 kbar) conditions related to the first deformation phase (D1) that generated vertical folds with associated foliation. These conditions evolved towards lower pressure and increasing temperature during the second phase (D2), which resulted from an extensional episode and produced sub-horizontal folds. A third folding phase (D3) resulted in subvertical folds and weak crenulation cleavage (Díez Balda *et al.* 1990; López-Plaza & Martínez Catalán 1987; Valle Aguado *et al.* 2005). Syn- to post-D3 metamorphic conditions largely erased earlier parageneses and only relics of staurolite, garnet and kyanite are preserved in some areas.

Biotite+fibrolite/sillimanite are characteristic minerals of the medium- and high-grade early metamorphic rocks, the folded (D3) migmatites, as well as the related leucogranites and two-mica granites. Peak metamorphic thermal conditions in different areas range from 800 ± 50 °C and 4–6 kbar (Barbero *et al.* 1995) to 700–740 °C and 2·5–3·5 kbar (Carnicero 1982; Escuder Viruete *et al.* 2000; Gil Ibarguchi & Martínez 1982; Ugidos 1987). In the study region, low-P metamorphism changed muscovite+biotite- and biotite+sillimanite-rich mineral assemblages into cordierite-rich (± andalusite ± sillimanite) parageneses in the high-grade metamorphic and anatectic rocks. Late in the deformation sequence, cordierite-

https://doi.org/10.1017/S1755691009008159 Published online by Cambridge University Press

**Table 1** Granite emplacement levels in relation stratigraphic units derived from sequence stratigraphy analysis in the Central Iberian Zone W and S of Salamanca (Valladares *et al.* 2000). The stratigraphic levels of some specific sample locations are also indicated.

| | Unit | Thickness (m) min. | Thickness (m) max. | Dominant lithology | Sequence stratigraphy | Granite emplacement level | Sample location |
|---|---|---|---|---|---|---|---|
| Lower Cambrian | XII | 180 | | sh/snd | Lowstands Systems Tract | BG, CBG; PayG; BVG, AG | |
| | XI | 100 | 260 | snd/sh/cong | | | SSA-8 |
| | X | 70 | 365 | sh | | | |
| | IX | 85 | 120 | sh/snd/cong | | | |
| | VIII | 120 | 240 | sh | | | SSA-7 & SSA-13 |
| | VII | 50 | 90 | cong/snd/sh | | | SIA-11 |
| | VI | 90 | 240 | sh | | | SSA-2 |
| | V | | 130 | calcareous breccia | | | |
| | | | | | SB | | PHA-1 & PHA-2 |
| Upper Neoproterozoic | IV | 40 | 500 | sh | h.s.t. / t.s.t. | | |
| | III | | 550 | sh/snd | Lowstand Systems Tract | | |
| | II | 225 | 600 | cong/sh | | | |
| | I | 97 | 585 | snd/sh | | | |
| | ? | | | | | | |
| | | | | Inferred sequence boundary | | | |

sh=shale; snd=sandstone; cong=conglomerate.
S.B.=sequence boundary; h.s.t.=high systems tract; t.s.t.=transgressive systems tract.
AG=amphibole-bearing biotite granite; BG=biotite granite; CBG=cordierite-bearing biotite granite; BVG=Bañobarez-Villavieja granite; PayG=El Payo granite.

rich rocks such as nebulitic diatexites, and spatially related high-grade hornfelses (pyroxene hornfels facies) and migmatitic hornfelses, were formed from two-mica schists and biotite+sillimanite migmatites in the thermal aureoles of late Variscan intrusive granites and related basic rocks (Franco & García de Figuerola 1986; Ugidos 1990). Granites are abundant in the CIZ and include amphibole-bearing biotite granites, biotite granites, cordierite-bearing biotite granites and cordierite-bearing two-mica granites. An ion microprobe age of ca. 306 Ma has been recently reported for biotite and cordierite-bearing biotite granodiorites and monzogranites in the area of this work (Zeck *et al.* 2007).

## 2. Analytical techniques

Representative samples of country host rocks, Upper Neoproterozoic shales and sandstones (including the highly altered reworked shales from the uppermost Neoproterozoic and lowermost Cambrian beds described above), and Lower Cambrian shales and nebulites were selected from the region into which the late Variscan granites were intruded. Additional samples of cordierite-bearing two-mica granites were collected to supplement existing datasets. Analyses were performed using ICP–AES (major elements) and ICP–MS (all other elements) techniques at the Service d'Analyses des Roches et Minéraux of the CRPG (Nancy, France). Samples were fused with $LiBO_2$ and dissolved in $HNO_3$.

A subset of samples were spiked with $^{87}Rb$, $^{84}Sr$, $^{145}Nd$ and $^{149}Sm$ and individual elements separated using methods similar to those described in Barbero *et al.* (1995). Sr samples were analysed on either a VG54E single collector thermal ionisation mass spectrometer or a VG Sector 54–30 multiple collector mass spectrometer operated in multi-dynamic mode. On both instruments, the $^{87}Sr/^{86}Sr$ ratio was corrected for mass fractionation using $^{86}Sr/^{88}Sr=0{\cdot}1194$ and an exponential law. For NIST SRM 987, the VG54E gave $^{87}Sr/^{86}Sr=0{\cdot}710230\pm116$ (2 s, n=43) and the VG Sector 54-30 mass spectrometer gave $0{\cdot}710246\pm20$ (2 s, n=14). Rb samples were analysed on either a VG MM30 single collector mass spectrometer or the VG54E instrument. Sm and Nd samples were analysed on the VG Sector 54-30 instrument. $^{143}Nd/^{44}Nd$ ratios were measured in multidynamic mode and corrected for mass fractionation using an exponential law and $^{146}Nd/^{144}Nd=0{\cdot}7219$. Repeat analyses of the internal laboratory standard (JM) gave $^{143}Nd/$

https://doi.org/10.1017/S1755691009008159 Published online by Cambridge University Press

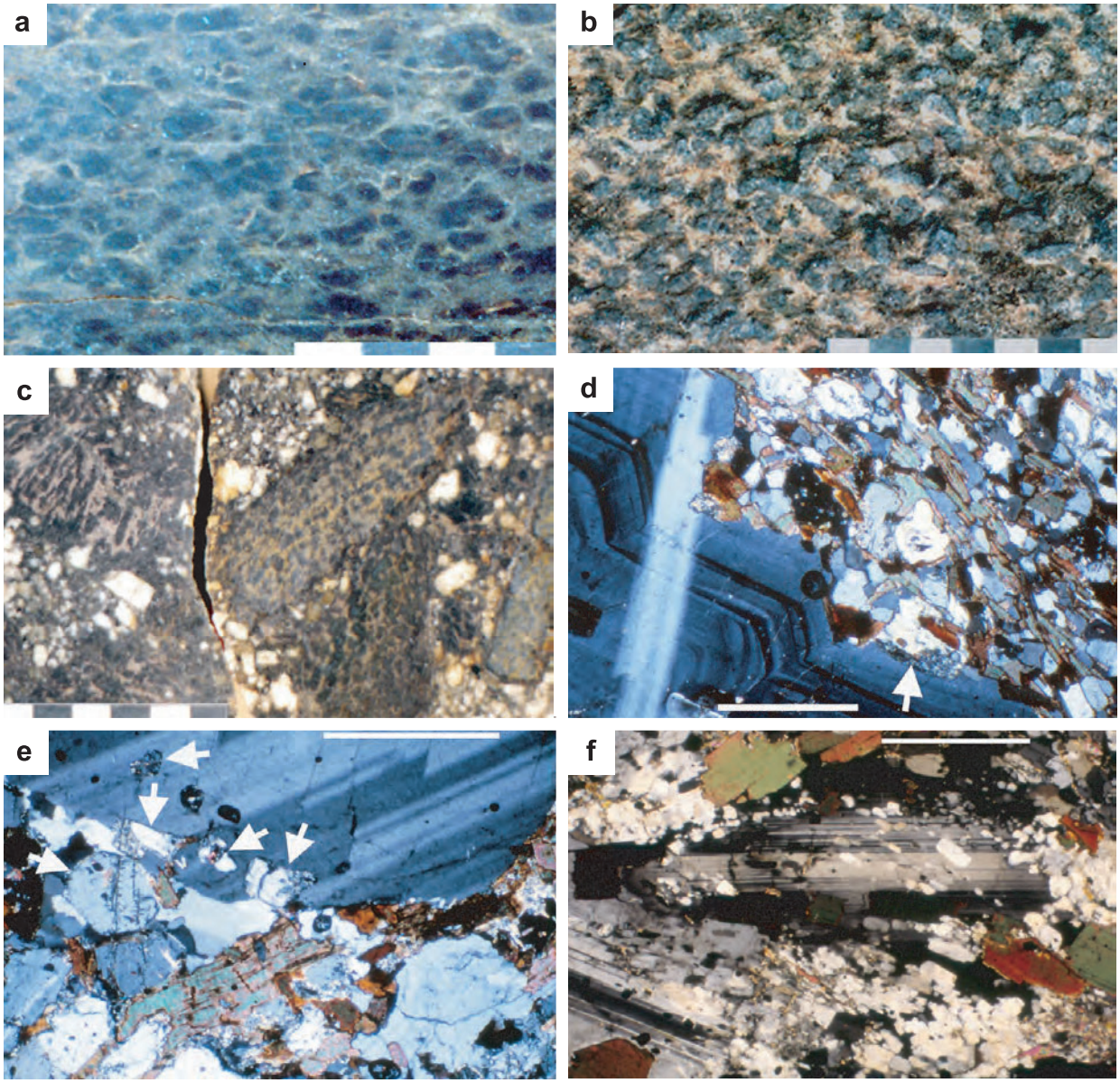


**Figure 2** Field images of low grade (a) and medium-grade (b) hornfelses with abundant cordierite. (c) Fragments of hornfels in biotite granite. (d) Photomicrographs of the contact between zoned plagioclase and hornfels, showing in (e) inclusions of cordierite crystals (arrows) in a plagioclase (same sample as (c)). (f) Cordierite crystals in a high-grade hornfels. Scales in cm for (a), (b) and (c); scale bars = 0·8 mm in (d), (e) and (f).

$^{144}Nd = 0{\cdot}511502 \pm 8$ (2 s, n = 9). Nd and Sm concentration (ID) runs were analysed in static mode.

Electron microprobe analyses were performed using a JEOL JCXA-733 instrument with a beam of 15 kV, 20 nA. Natural mineral and pure metal standards were used for calibration and apparent concentrations were corrected using the ZAF method.

## 3. Petrography

### 3.1. High-grade hornfelses

These are characterised by phyllosilicate-consuming reactions forming cordierite, sillimanite and K-feldspar in the aureoles of some biotite granites, locally accompanied by the inversion of fibrolite to andalusite. Cordierite crystals range from anhedral to euhedral and usually contain inclusions of sillimanite or andalusite prisms, although some lack inclusions. In other examples, numerous inclusion-free cordierite prisms have replaced the foliation defined by phyllosilicates and the resulting hornfelses show alternating felsic and cordierite-rich levels. Migmatitic hornfelses with leucocratic veins have been described (García de Figuerola & Franco 1975; Franco & García de Figuerola 1986; Ugidos *et al.* 1990). Field and textural aspects are illustrated in Figures 2, 3 and 4.

### 3.2. Nebulites

The anatectic country rocks, mainly diatexites, are characterised by their relatively high abundance of cordierite (in general 10–20% modal) forming embayed to euhedral crystals (Figs 3, 4) with or without biotite and/or fibrolite inclusions, and are petrographically equivalent to cordierite-rich granodiorites. However, the term nebulite is preferred for clarity to distinguish these autochthonous rocks from clearly intrusive cordierite-bearing granites. In the field, nebulites have a characteristic deep grey-blue colour, with variable amounts of relict biotite + sillimanite and relatively abundant enclaves of refractory material, such as disrupted beds of quartzite, marble and calc-silicate rocks. Some microgranular rocks, gneisses, relicts of deformed migmatites, and associated leucogranites

https://doi.org/10.1017/S1755691009008159 Published online by Cambridge University Press

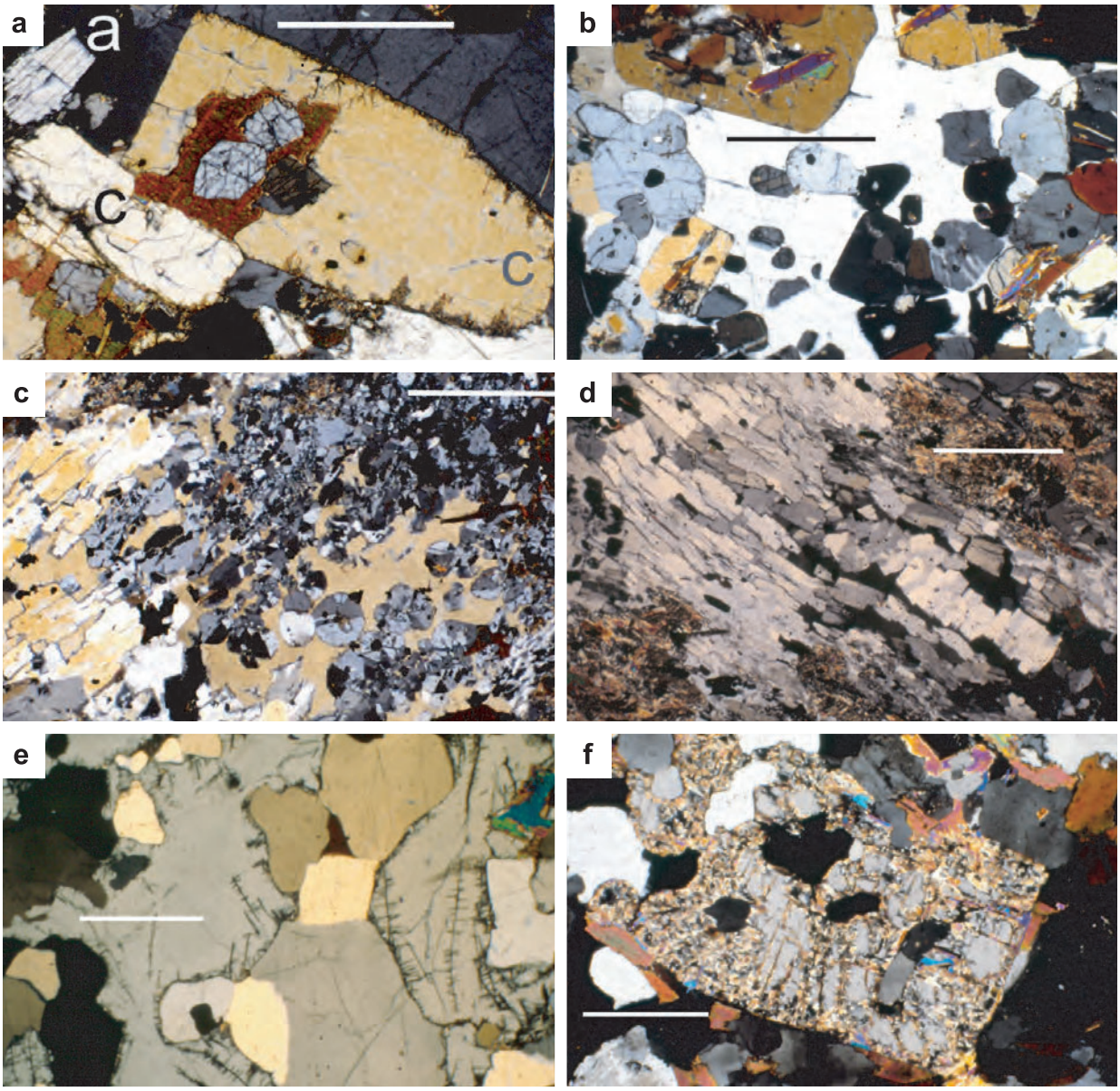


**Figure 3** Photomicrograph of a high grade hornfels showing (a) andalusite and biotite included in cordierite (labelled c), with andalusite (labelled a) occurring as an independent crystal. (b) Cordierite crystals with and without sillimanite inclusions in an enclave of migmatitic hornfels. (c) and (d) Textures of cordierite in high-grade hornfelses. (e) and (f) Textures of cordierite in nebulites. Scale bars=0·8mm.

are also present. Undeformed leucogranites, representing less than 5% of the exposed rocks, are also present in the nebulites as dykes up to 20–30 cm thick and less than 10 m long, and as isolated outcrops of less than 1 $m^2$. These consist of quartz, oligoclase-albite, alkali feldspar and accessory minerals such as cordierite, biotite, tourmaline and fibrolite. No clear cross-cutting relationships have been observed for the nebulites and boundaries with other (folded) biotite+sillimanite-rich migmatites are transitional. Rocks comparable to nebulites are the nebulitic diatexites reported in the Bohemian Massif (Finger & Clemens 1995), in the Central Damara Orogen (Jung *et al.* 2000), and the diatexites of the Cooma Suite (Healy *et al.* 2004).

### 3.3. Cordieritites

Cordieritites (with >60% cordierite) are uncommon rocks, and are generally considered restites following the removal of leucogranite melts (see below). In the present study area, a cordieritite macro-enclave outcrops over several square metres within the biotite granite and has been cored for up to 10 m in depth without crossing the lower contact with the host granite. The enclave is coarse-grained and mostly consists of whole pinitised cordierite prisms (60–80%) up to 3–4 cm in diameter, inclusion-free andalusite grains up to 5–6 mm in diameter (Figs 4, 5), quartz, muscovite, chlorite, apatite and opaques. The host granite outcrops over hundreds of $km^2$, but only contains cordierite prisms (Fig. 4) and muscovite when in close proximity to the cordieritite (Ugidos 1988). Another enclave of cordieritite, also several square metres in outcrop, has been found in a cordierite-bearing ($\pm$ muscovite, $\pm$ andalusite, $\pm$ fibrolite) biotite granite. This is a medium-grained rock with the same mineralogy and texture as the coarse-grained cordieritite. Other enclaves at this locality are cordierite-rich (>40 vol. %) hornfelses.

### 3.4. Granites *s.l.*

Much has been written on the late Variscan granites (mostly monzogranites and granodiorites) of the present study area and only a summary of their characteristics is presented here.

https://doi.org/10.1017/S1755691009008159 Published online by Cambridge University Press

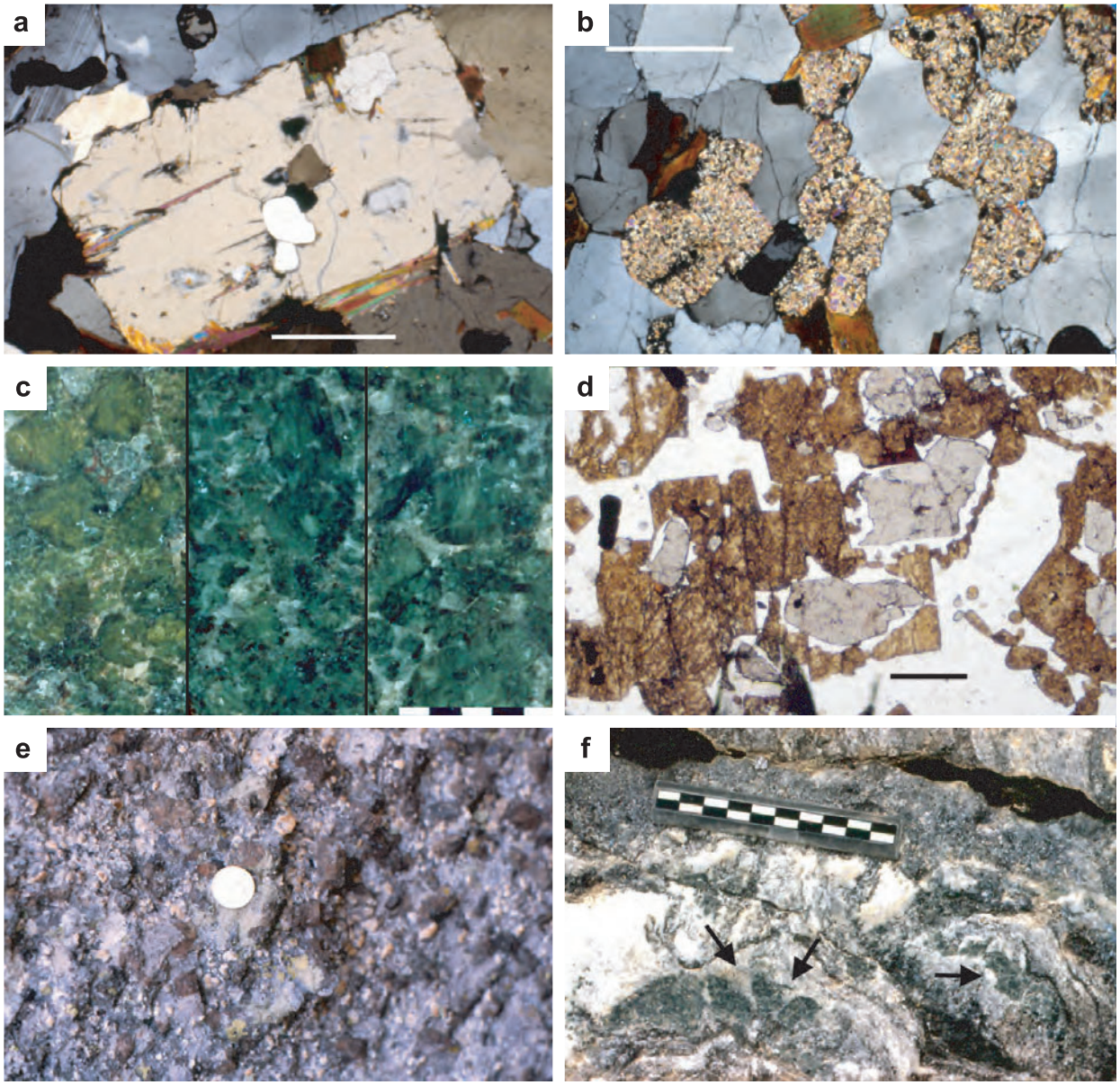


**Figure 4** (a) and (b) photomicrographs illustrating the textures of cordierite in nebulites. (c) Drill cores of a cordieritite enclave in a biotite granite taken from depths of 4 m, 9 m and 10·5 m (left to right respectively). (d) Photomicrograph of cordierite (pinitised) and andalusite in a cordieritite enclave from a cordierite (±andalusite ±fibrolite)-bearing granite. (e) Cordierite-bearing granite close to the cordieritite enclave of (c). Diameter of the coin is 2·5 cm. (f) Cordierite prisms (arrows) replacing restitic (mostly biotite+sillimanite) minerals in a roof pendant within cordierite-bearing granite. Scale bars=0·8mm; rulers marked in cm.

The quantitatively most abundant types include amphibole-bearing biotite granites, biotite granites, cordierite-bearing biotite granites and cordierite (±andalusite)-bearing two-mica granites. Each type intrudes both the Upper Neoproterozoic and the Lower Cambrian sedimentary series, and all except the amphibole-bearing biotite granites are in part hosted by high grade metamorphic and anatectic rocks. The amphibole-bearing granites have allanite and titanite as accessory phases and show a gradual transition to the biotite granites. Representative areas of these granites have been studied by various authors (Fernández *et al*. 1982; Hernández *et al*. 1982; Franco & Sánchez 1987; Ugidos 1988; Ugidos *et al*. 1990; Moreno-Ventas *et al*. 1995). The biotite granites have a gradual transition into the cordierite-bearing biotite granites and the abundance of cordierite (as pinitised prisms generally up to 1–1·5 cm, maximum 3 cm in diameter; pinitisation is complete in most crystals and only scarce partially-fresh cordierite prisms have been found) ranges from >20 prisms/m$^2$ (maximum 74 prisms/m$^2$) to <1 prism/m$^2$ in the marginal and internal facies, respectively (Ugidos & Recio 1993). The textural features of cordierite are identical to those found in the high-grade host rocks, nebulites, and cordieritites. Microgranular enclaves with cordierite prisms up to 1·5 cm and, more rarely, andalusite and fibrolite, are present in the marginal cordierite-bearing granites (Martín *et al*. 1990; Ugidos 1988, 1990).

Enclaves of basic to tonalitic rocks are frequent in the amphibole-bearing, biotite and cordierite-bearing granites (Ugidos *et al*. 1988; Martín *et al*. 1990; Moreno-Ventas *et al*. 1995). Enclaves of metamorphic rocks such as schists and low-to-medium grade hornfelses are present in amphibole-bearing and biotite granites near their contacts with the country rocks. High-grade host rocks, such as hornfelses, gneisses, folded migmatites and nebulites, are common enclaves in some areas of the cordierite-bearing granites, but are absent in amphibole-bearing and biotite granites. Rafts up to 6 km$^2$, mainly consisting of these rocks and early Variscan leucogranites and their associated restitic mesosomes (Fig. 4),

https://doi.org/10.1017/S1755691009008159 Published online by Cambridge University Press

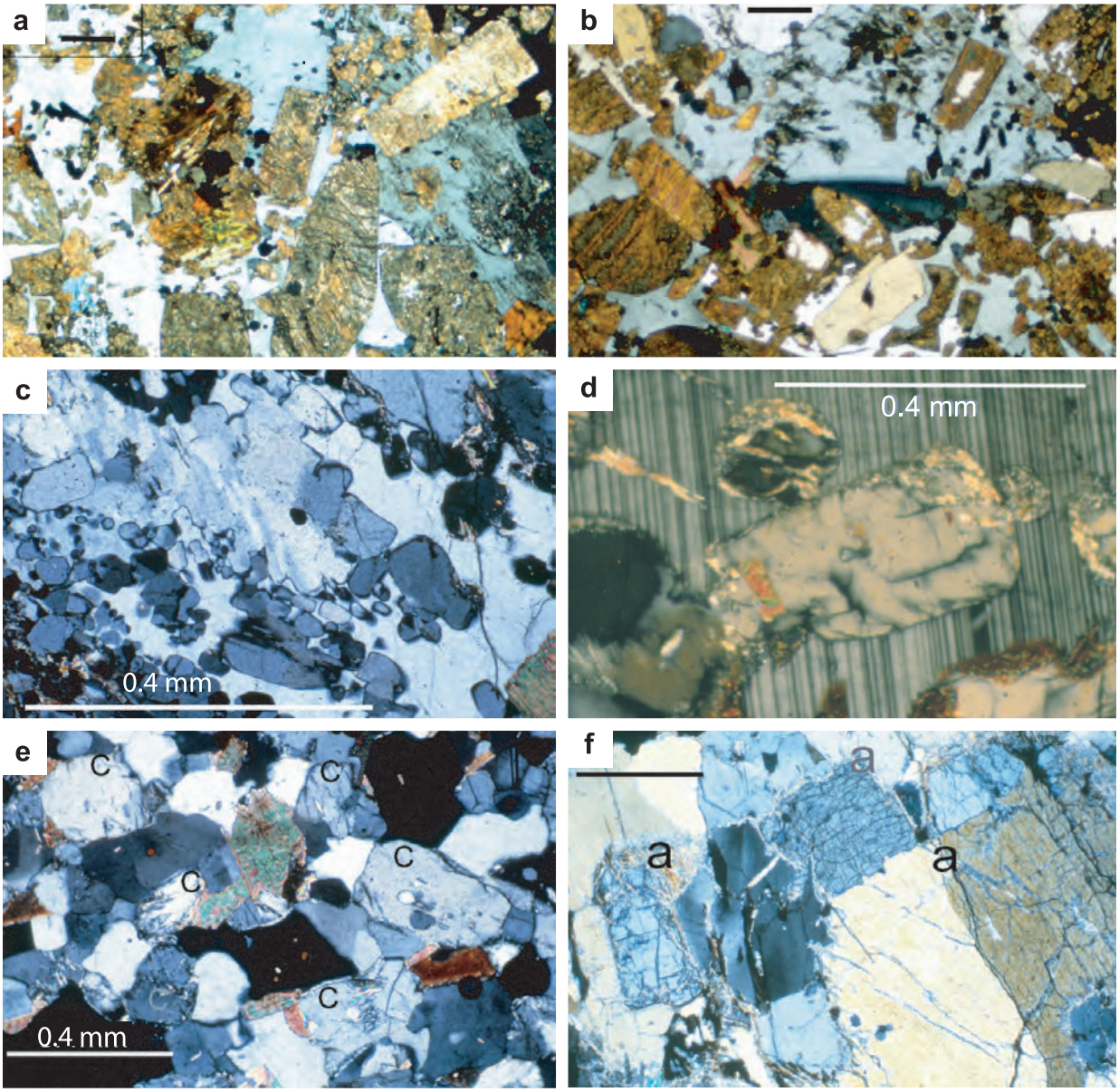


**Figure 5** Photomicrographs (a) and (b) of cordierite (pinitised) and andalusite in a cordieritite. (c), (d) and (e) cordierite in a high-grade hornfels. (f) Andalusite (labelled a) in the cordieritite of Figure 4c. Scale bars in (a), (b) and (f)=0·8mm.

are especially abundant E of Barco de Avila-Navalonguilla (Fig. 1) in the Gredos Massif (Odriozola *et al.* 1981a, b). Gradual transitions between the biotite granites and cordierite-bearing granites and transitional contacts between these late granites and the nebulites are regional features reported in various areas (Carracedo *et al.* 1989; Ugidos *et al.* 1990; Moreno-Ventas *et al.* 1995).

Representative cordierite-bearing two mica granites to the W and SW of Salamanca (Fig. 1) include the Bañobarez-Villavieja granites (Carnicero *et al.* 1987; López-Plaza & Carnicero 1987). These and the El Payo granite intrude the medium-grade metamorphosed Lower Cambrian series and the (García de Figuerola *et al.* 1988). Typically these granite bodies have cordierite, fibrolite and andalusite. SE of Salamanca the small Bohoyo and Navalonguilla granite bodies (Fig. 1) of cordierite-bearing two mica granite types have minor cordierite and sillimanite (Odriozola *et al.* 1981a).

Plagioclase compositions (core and rim) in the host metamorphic rocks vary from $An_{51}$ to $An_{14}$ (mean $An_{31}$), whereas associated nebulite plagioclase compositions are more sodic, in the range $An_{35}$ to $An_{6}$ (mean $An_{22}$). There is near complete overlap between these nebulite feldspars and those in the cordierite granite ($An_{35}$ to $An_{9}$, mean $An_{23}$) and a shift to slightly more anorthitic compositions in the biotite granites (range $An_{46}$ to $An_{12}$, mean $An_{28}$). There is no significant difference in the composition of cordierite in representative samples of the cordierite granites and the nebulites for Mg# ($55{\cdot}5 \pm 2{\cdot}8$, seven samples, 38 point analyses and $55{\cdot}9 \pm 5{\cdot}0$, six samples, 56 point analyses respectively, all 2 s) whereas Mg# in the metamorphic rocks is slightly higher but rather more dispersed ($58{\cdot}8 \pm 10{\cdot}8$, 14 samples, 104 points). Na is the only element in cordierite that shows a significant difference, being higher in the granites than the nebulites ($0{\cdot}104 \pm 0{\cdot}084$ per formula unit and $0{\cdot}064 \pm 0{\cdot}048$, respectively, $r<0{\cdot}01$).

## 4. Whole rock geochemistry

### 4.1. Major and trace elements

**4.1.1. Unmetamorphosed country rocks and nebulites.** Representative compositions of Upper Neoproterozoic shales and sandstones and Lower Cambrian shales are presented in Table

https://doi.org/10.1017/S1755691009008159 Published online by Cambridge University Press

**Table 2** Representative analyses of Upper Neoproterozoic and Lower Cambrian detrital country rocks S of Salamanca (Central Iberian Zone).

| | 1 | 1 | 1 | 2 | 2 | 2 | 3 | 3 | 3 | 4 | 4 | 4 |
|---|---|---|---|---|---|---|---|---|---|---|---|---|
| Sample | SIA-25 | SIA-24 | SSA-12 | SIA-9 | SIA-23 | SIA-32 | SSA-16 | SSA-17 | GUA-31 | SSA-2 | SIA-11 | SSA-13 |
| $SiO_2$ | 59·32 | 61·59 | 56·07 | 71·62 | 72·97 | 75·82 | 60·15 | 58·86 | 58·61 | 60·45 | 58·73 | 55·86 |
| $TiO_2$ | 0·93 | 1·04 | 1·10 | 0·73 | 0·68 | 0·45 | 0·86 | 0·67 | 0·73 | 0·93 | 0·77 | 1·00 |
| $Al_2O_3$ | 20·0 | 18·90 | 20·86 | 13·13 | 12·33 | 8·89 | 20·34 | 19·30 | 19·92 | 19·88 | 19·92 | 21·46 |
| $Fe_2O_3$ | 7·36 | 6·03 | 8·36 | 5·33 | 5·06 | 4·71 | 6·94 | 5·66 | 7·52 | 5·81 | 7·28 | 8·41 |
| MnO | 0·04 | 0·04 | 0·07 | 0·02 | 0·04 | 0·10 | 0·08 | 0·04 | 0·08 | 0·04 | 0·08 | 0·07 |
| MgO | 2·51 | 2·06 | 2·85 | 1·76 | 1·62 | 2·30 | 2·28 | 2·85 | 3·03 | 2·05 | 3·09 | 2·86 |
| CaO | 0·20 | 0·37 | 0·26 | 0·17 | 0·76 | 1·36 | 0·15 | 0·36 | 0·58 | 0·37 | 0·07 | 0·49 |
| $Na_2O$ | 1·56 | 1·88 | 0·87 | 1·45 | 2·22 | 1·44 | 0·27 | 1·71 | 1·24 | 1·03 | 0·24 | 1·23 |
| $K_2O$ | 3·58 | 3·94 | 3·46 | 2·26 | 1·79 | 1·02 | 4·11 | 3·67 | 3·99 | 4·37 | 3·78 | 3·26 |
| $P_2O_5$ | 0·14 | 0·18 | 0·31 | 0·15 | 0·11 | 0·08 | 0·17 | 0·09 | 0·11 | 0·21 | 0·19 | 0·17 |
| LOI | 4·08 | 3·67 | 5·47 | 3·16 | 2·19 | 3·78 | 4·35 | 6·67 | 4·11 | 4·72 | 5·60 | 5·01 |
| total | 99·72 | 99·70 | 99·68 | 99·78 | 99·77 | 99·95 | 99·70 | 99·88 | 99·92 | 99·86 | 99·75 | 99·82 |
| Rb | 135 | 114 | 123 | 86 | 68 | 36 | 171 | 160 | 170 | 183 | 149 | 133 |
| Cs | 8·6 | 3·6 | 9·0 | 4·0 | 5·0 | 1·5 | 8·7 | 8·7 | 7·6 | 8·9 | 8·4 | 10·4 |
| Be | 2·6 | 1·9 | 2·7 | 1·7 | 2·5 | 0·8 | 3·5 | 3·2 | 4·0 | 3·2 | 3·0 | 3·0 |
| Sr | 84 | 57 | 139 | 64 | 109 | 36 | 80 | 94 | 94 | 127 | 66 | 144 |
| Ba | 603 | 728 | 669 | 412 | 341 | 180 | 637 | 861 | 868 | 741 | 612 | 694 |
| La | 39·1 | 38·2 | 51·7 | 31·0 | 30·0 | 23·9 | 45·0 | 30·0 | 37·0 | 68·5 | 30·0 | 54·3 |
| Ce | 78·7 | 81·8 | 112 | 69·1 | 67·3 | 54·9 | 90·8 | 59·3 | 73·9 | 127 | 56·4 | 96·8 |
| Pr | 9·79 | 9·52 | 13·7 | 7·55 | 7·07 | 5·43 | 10·6 | 7·05 | 8·89 | 18·8 | 8·68 | 16·6 |
| Nd | 36·8 | 38·5 | 56·3 | 29·7 | 27·4 | 20·4 | 40·5 | 27·9 | 31·9 | 78·6 | 40·8 | 78·3 |
| Sm | 7·96 | 8·32 | 12·0 | 5·81 | 5·88 | 4·29 | 7·60 | 5·49 | 6·39 | 16·4 | 8·78 | 18·1 |
| Eu | 1·63 | 1·62 | 2·48 | 1·39 | 1·23 | 0·94 | 1·54 | 1·32 | 1·23 | 3·95 | 2·10 | 4·26 |
| Gd | 6·19 | 6·90 | 10·2 | 5·06 | 4·53 | 3·50 | 6·76 | 4·68 | 4·56 | 18·7 | 10·5 | 20·5 |
| Tb | 1·02 | 1·12 | 1·51 | 0·80 | 0·72 | 0·52 | 1·05 | 0·79 | 0·72 | 3·51 | 1·81 | 2·98 |
| Dy | 5·83 | 6·51 | 8·62 | 4·45 | 4·09 | 3·02 | 5·98 | 4·78 | 4·12 | 22·0 | 11·8 | 18·7 |
| Ho | 1·21 | 1·41 | 1·84 | 0·96 | 0·84 | 0·67 | 1·33 | 0·91 | 0·88 | 5·40 | 3·15 | 4·42 |
| Er | 3·28 | 3·70 | 4·55 | 2·40 | 2·31 | 1·75 | 3·60 | 2·70 | 2·36 | 13·1 | 8·10 | 11·62 |
| Tm | 0·49 | 0·58 | 0·72 | 0·34 | 0·34 | 0·26 | 0·53 | 0·46 | 0·39 | 1·97 | 1·18 | 1·80 |
| Yb | 3·28 | 3·99 | 4·54 | 2·59 | 2·29 | 1·78 | 3·53 | 3·16 | 2·42 | 12·1 | 8·03 | 11·0 |
| Lu | 0·51 | 0·58 | 0·63 | 0·33 | 0·37 | 0·27 | 0·54 | 0·49 | 0·42 | 1·59 | 1·16 | 1·54 |
| (La/Yb)*n* | 8·1 | 6·5 | 7·7 | 8·1 | 8·9 | 9·1 | 8·6 | 6·4 | 10 | 3·8 | 2·5 | 3·3 |
| Eu/Eu* | 0·71 | 0·65 | 0·68 | 0·78 | 0·73 | 0·74 | 0·66 | 0·80 | 0·70 | 0·69 | 0·67 | 0·68 |
| Y | 34 | 38 | 46 | 25 | 24 | 18 | 37 | 27 | 25 | 173 | 105 | 138 |
| Zr | 209 | 260 | 245 | 216 | 253 | 200 | 168 | 152 | 137 | 230 | 165 | 237 |
| Th | 11·2 | 12·7 | 13·3 | 8·5 | 8·2 | 6·7 | 14·1 | 10·7 | 14·8 | 12·6 | 11·0 | 14·0 |
| U | 3·6 | 3·2 | 4·1 | 2·4 | 2·5 | 1·6 | 3·7 | 3·7 | 3·5 | 3·8 | 3·0 | 4·0 |
| V | 128 | 130 | 146 | 82 | 77 | 45 | 121 | 137 | 126 | 135 | 113 | 148 |
| Nb | 13 | 14 | 15 | 11 | 9 | 7 | 15 | 11 | 12 | 15 | 12 | 15 |
| Cr | 105 | 113 | 133 | 78 | 75 | 47 | 103 | 105 | 97 | 115 | 102 | 135 |
| Co | 19 | 18 | 14 | 25 | 31 | 37 | 10 | 24 | 28 | 9 | 11 | 10 |
| Ni | 48 | 35 | 22 | 33 | 30 | 22 | 39 | 73 | 53 | 20 | 47 | 25 |
| Mg# | 40 | 40 | 40 | 40 | 39 | 49 | 39 | 50 | 44 | 41 | 46 | 40 |
| Ti/Nb | 422 | 457 | 500 | 405 | 445 | 409 | 350 | 370 | 356 | 382 | 382 | 396 |
| Rb/Sr | 1·61 | 2·00 | 0·88 | 1·34 | 0·62 | 1·00 | 2·14 | 1·70 | 1·80 | 1·46 | 2·26 | 0·92 |
| Sr/Ba | 0·14 | 0·08 | 0·21 | 0·16 | 0·32 | 0·20 | 0·13 | 0·11 | 0·11 | 0·17 | 0·11 | 0·21 |
| Rb/Zr | 0·65 | 0·44 | 0·50 | 0·40 | 0·27 | 0·18 | 1·02 | 1·05 | 1·24 | 0·80 | 0·90 | 0·56 |
| Ce/Ce* | 0·94 | 1·01 | 0·99 | 1·06 | 1·08 | 1·13 | 0·98 | 0·96 | 0·96 | 0·83 | 0·82 | 0·76 |
| Sm/Nd | 0·217 | 0·216 | 0·213 | 0·195 | 0·215 | 0·211 | 0·188 | 0·197 | 0·201 | 0·209 | 0·215 | 0·231 |

1 and 2, Upper Neoproterozoic shales and sandstones, respectively; 3, Lower Cambrian shales; 4, altered Lower Cambrian shales.
Major elements in weight %; trace elements in ppm; *n*: chondrite (Taylor & McLennan 1985) normalised.
Eu/Eu*: Eu*n*/(Sm*n* × Gd*n*)$^{1/2}$; Mg#: [MgO/(MgO+FeO)] × 100; Ce/Ce*: Ce*n*/(La*n* × Pr*n*)$^{1/2}$.

2. Also included are three representative analyses of shales from above the Upper Neoproterozoic–Lower Cambrian unconformity that show evidence of REE redistribution. Complete analytical data for 65 shale and 15 sandstone samples have been published (Ugidos *et al.* 1997a, 2003a, b). These country rocks are characterised by a) relatively low CaO and $Na_2O$ contents and the shales and sandstones have essentially the same Mg#; and b) significant chemical differences between the Upper Neoproterozoic and Lower Cambrian shales, including $TiO_2$ and Zr abundances and Rb/Zr, Ti/Nb ratios and $\varepsilon_{Nd}$ values (Ugidos *et al.* 1997b, 2003a; Valladares *et al.* 2002b). The reworked shales have the highest HREE (heavy rare earth elements; LREE, light rare earth elements) and Y contents, the lowest $(La/Yb)_n$ ratios and negative cerium

https://doi.org/10.1017/S1755691009008159 Published online by Cambridge University Press

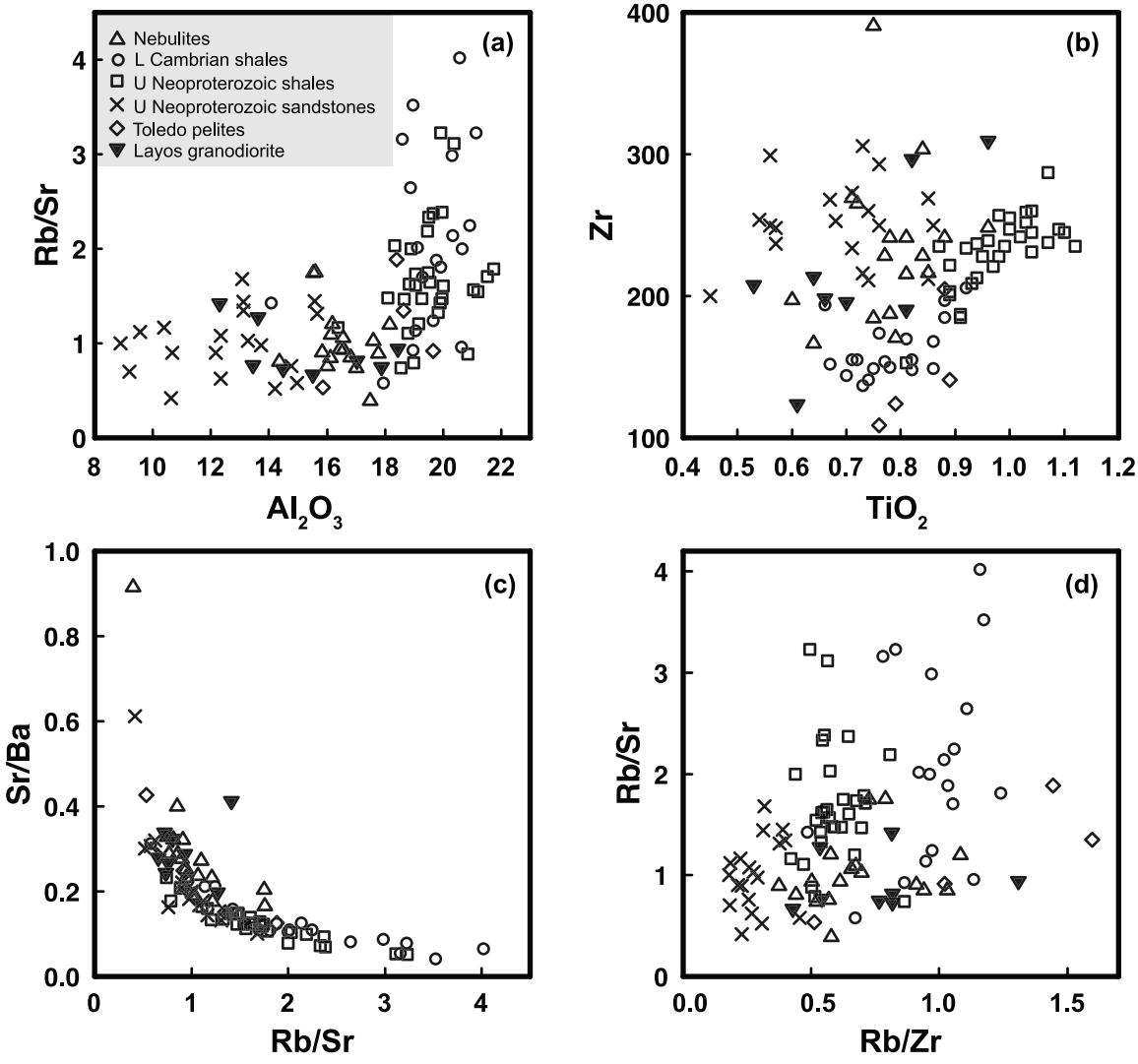


**Figure 6** Variation diagrams comparing country sedimentary rocks, nebulites and the Layos granodiorite. Data for Layos granodiorite and Toledo pelites from Barbero & Villaseca (1992) and Barbero *et al.* (1995).

anomalies. Analyses of nebulites are shown in Table 3, and also included is the average Layos granodiorite from the Toledo area, an anatectic residuum-rich rock 'characterised by a high modal proportion of cordierite (up to 30%)'. Cordierite in this granite 'usually occurs as euhedral or subhedral grains with frequent inclusions of acicular sillimanite, biotite and quartz'. Enclaves of metamorphic country rocks (orthogneisses, amphibolites, quartzitic conglomerates, calcsilicate rocks and marbles) are the most abundant, followed by cordierite-rich and sillimanite-rich enclaves and mafic igneous enclaves (amphibole–biotite-bearing quartz diorites and gabbros) (Barbero & Villaseca 1992; Barbero *et al.* 1995). Nebulites have higher CaO contents (>0·5%) than shales and sandstones and Eu/Eu* ranges from 0·52 to 0·96. The range of whole rock Mg# (37–44) in nebulites and Layos granodiorite (31–43) are comparable with those of the shales and sandstones. CaO contents and Eu/Eu* in the Layos granodiorite (Barbero & Villaseca 1992; Barbero *et al.* 1995) are in the same range as the nebulites.

The nebulites generally have compositions intermediate between the Upper Neoproterozoic shales and sandstones and overlap the Lower Cambrian shales, as shown by $Al_2O_3$–Rb/Sr, $TiO_2$–Zr, Rb/Sr–Sr/Ba, and Rb/Zr–Rb/Sr variation diagrams (Fig. 6a–d, note that samples showing evidence of REE redistribution are not included in these plots). Moreover, the shales, sandstones, nebulites and the Layos granodiorite all follow the same trend in the Rb/Sr–Sr/Ba diagram and all have similar ranges of Rb/Sr, Rb/Zr and Sr/Ba (Fig. 6a, c, d). Thus, the chemical data indicate that the nebulites and the Layos granodiorite have strong major and trace element affinities with the Upper Neoproterozoic and Lower Cambrian metasedimentary rocks, and the simplest explanation is that the nebulites and the Layos granodiorite are anatectic residuum-rich rocks equivalents of unfractionated metasedimentary material. This general conclusion does not exclude possible chemical variations on a local scale as a consequence of an accumulation of small volumes of leucocratic melts. Table 3 contains three analyses of a leucogranite in the nebulites. This granite type is characterised by high K/Rb (326–357) and Eu/Eu* (3·2–16·3), with low $(La/Yb)_n$ (2·6–4·2). These features preclude an origin through magmatic fractionation, rather they suggest local fluid-present melting of the quartz, plagioclase and alkali feldspar components of nebulites, without the contribution of other minerals. Similar Rb/Sr and Sr/Ba ratios in the nebulites and leucogranites support this interpretation.

**4.1.2. Cordieritites and related rocks.** Analytical data for the cordieritites, two chemically anomalous sedimentary rocks, and two phosphate-rich rocks are presented in Table 4. The cordieritites show relatively high $P_2O_5$, MnO, Cs and Be and low $TiO_2$, but they share, together with samples SSA-7 (sandstone) and SSA-8 (shale), some important chemical features, such as low contents of V, Cr, Ni, Cu, and low Eu/Eu* ratios.

https://doi.org/10.1017/S1755691009008159 Published online by Cambridge University Press

**Table 3** Analyses of nebulites and associated leucogranites S of Salamanca (Central Iberian Zone).

| Sample | NB I-25 | NB I-30 | NB ABE-1 | NB ABE-2 | NB ABE-3 | NB ABE-4 | NB BOA-4 | NB BOA-5 | NB BOA-6 | NB VAA-9 | NB PHU-2 | NB PHU-4 | NB PHU-5 | NB JAM-2 | NB BEU-32 | NB BEU-33 | NB JUM-1 | LG JUM-2 | LG BEU-40 | LG PHU-26 | Layos $n=8$ |
|---|---|---|---|---|---|---|---|---|---|---|---|---|---|---|---|---|---|---|---|---|---|
| $SiO_2$ | 69·5 | 65·96 | 66·34 | 66·75 | 63·85 | 63·51 | 63·46 | 66·09 | 66·03 | 61·43 | 66·3 | 65·55 | 61·82 | 65·17 | 67·31 | 67·19 | 64·52 | 74·61 | 73·61 | 73·79 | 67·19 |
| $TiO_2$ | 0·84 | 0·96 | 0·60 | 0·64 | 0·85 | 0·81 | 0·75 | 0·81 | 0·75 | 0·79 | 0·77 | 0·78 | 0·88 | 0·78 | 0·72 | 0·71 | 0·84 | 0·04 | 0·02 | 0·04 | 0·72 |
| $Al_2O_3$ | 14·36 | 16·44 | 15·84 | 16·11 | 16·58 | 17·02 | 17·77 | 16·55 | 16·82 | 18·16 | 16·01 | 16·14 | 17·48 | 17·60 | 15·54 | 15·59 | 16·18 | 13·93 | 14·73 | 14·73 | 15·34 |
| $Fe_2O_3$ | 6·03 | 6·74 | 4·91 | 4·97 | 6·77 | 6·43 | 6·75 | 6·30 | 5·32 | 6·72 | 5·66 | 5·80 | 6·73 | 6·22 | 4·69 | 4·39 | 5·46 | 0·51 | 0·30 | 0·71 | 5·69 |
| MnO | 0·07 | 0·06 | 0·07 | 0·08 | 0·08 | 0·07 | 0·09 | 0·07 | 0·06 | 0·08 | 0·06 | 0·04 | 0·07 | 0·05 | 0·03 | 0·03 | 0·02 | b.d. | b.d. | b.d. | 0·08 |
| MgO | 1·79 | 2·19 | 1·80 | 1·62 | 2·73 | 2·03 | 2·38 | 2·00 | 1·76 | 2·47 | 1·87 | 1·82 | 2·66 | 1·79 | 1·42 | 1·40 | 1·63 | 0·14 | 0·04 | 0·29 | 1·87 |
| CaO | 0·95 | 0·63 | 1·02 | 1·32 | 0·70 | 0·95 | 1·21 | 0·68 | 1·14 | 1·04 | 1·37 | 1·35 | 2·58 | 0·55 | 1·55 | 1·47 | 1·86 | 0·86 | 0·77 | 0·85 | 1·01 |
| $Na_2O$ | 2·15 | 1·95 | 2·67 | 2·77 | 2·53 | 2·68 | 2·45 | 2·11 | 2·48 | 2·36 | 2·56 | 2·52 | 3·16 | 2·15 | 2·86 | 2·69 | 2·91 | 3·08 | 2·78 | 2·87 | 2·34 |
| $K_2O$ | 2·13 | 3·15 | 3·86 | 3·64 | 3·26 | 3·18 | 3·56 | 3·45 | 4·29 | 3·86 | 3·25 | 3·97 | 2·58 | 3·65 | 4·11 | 4·63 | 4·44 | 5·68 | 7·00 | 5·45 | 3·66 |
| $P_2O_5$ | 0·14 | 0·16 | 0·18 | 0·22 | 0·28 | 0·27 | 0·20 | 0·17 | 0·28 | 0·14 | 0·30 | 0·38 | 0·40 | 0·17 | 0·34 | 0·42 | 0·32 | 0·19 | 0·14 | 0·20 | 0·30 |
| LOI | 1·62 | 1·32 | 1·25 | 1·22 | 1·64 | 1·64 | 1·72 | 1·97 | 1·30 | 1·60 | 1·33 | 1·37 | 1·33 | 1·58 | 1·15 | 1·19 | 1·53 | 0·73 | 0·50 | 0·91 | 1·63 |
| total | 99·58 | 99·56 | 98·54 | 99·34 | 98·89 | 98·59 | 100·3 | 100·2 | 100·2 | 98·65 | 99·48 | 99·72 | 99·69 | 99·71 | 99·72 | 99·71 | 99·71 | 99·77 | 99·89 | 99·84 | 99·64 |
| Rb | 101 | 125 | 180 | 172 | 133 | 126 | 146 | 142 | 174 | 185 | 130 | 163 | 140 | 131 | 193 | 213 | 175 | 132 | 165 | 139 | 150 |
| Sr | 124 | 132 | 197 | 201 | 141 | 169 | 162 | 133 | 203 | 153 | 170 | 148 | 352 | 127 | 110 | 121 | 144 | 108 | 264 | 195 | 174 |
| Ba | 382 | 564 | 610 | 501 | 555 | 512 | 583 | 559 | 699 | 653 | 584 | 539 | 384 | 661 | 534 | 722 | 807 | 425 | 1008 | 634 | 618 |
| La | 27·8 | 40·6 | 36·0 | 48·6 | 37·9 | 43·7 | 51·8 | 36·0 | 45·4 | 49·2 | 38·6 | 41·4 | 43·5 | 32·9 | 40·8 | 41·4 | 51·6 | 4·69 | 1·76 | 4·17 | 35·0 |
| Ce | 61·6 | 83·4 | 70·1 | 69·8 | 68·4 | 86·8 | 102 | 73·5 | 90·0 | 95·4 | 80·0 | 90·1 | 92·9 | 70·2 | 89·4 | 93·8 | 113 | 8·98 | 2·86 | 8·14 | 71·3 |
| Pr | n.a. | n.a. | n.a. | n.a. | n.a. | n.a. | n.a. | n.a. | n.a. | n.a. | n.a. | n.a. | n.a. | n.a. | 10·9 | 11·6 | 13·6 | 1·02 | 0·31 | 0·97 | n.a. |
| Nd | 25·7 | 33·9 | 27·4 | 26·6 | 29·2 | 38·3 | 40·5 | 29·9 | 35·7 | 35·7 | 33·9 | 41·5 | 40·0 | 30·9 | 44·5 | 46·0 | 54·2 | 4·18 | 1·01 | 3·66 | 32·8 |
| Sm | 6·10 | 7·21 | 6·19 | 6·13 | 6·95 | 8·07 | 9·31 | 6·37 | 7·75 | 8·17 | 7·76 | 8·94 | 8·06 | 6·79 | 9·50 | 9·59 | 10·9 | 0·99 | 0·24 | 1·03 | 7·39 |
| Eu | 1·65 | 1·34 | 1·43 | 1·22 | 1·69 | 1·66 | 1·64 | 1·27 | 1·48 | 1·86 | 1·28 | 1·37 | 1·45 | 1·53 | 1·39 | 1·53 | 1·67 | 1·26 | 1·27 | 1·15 | 1·29 |
| Gd | 4·51 | 5·12 | 4·35 | 4·50 | 5·24 | 5·46 | 6·98 | 4·27 | 5·36 | 6·06 | 5·93 | 6·79 | 5·76 | 5·52 | 6·77 | 7·17 | 8·72 | 0·86 | 0·23 | 1·21 | 6·34 |
| Tb | n.a. | n.a. | n.a. | n.a. | n.a. | n.a. | n.a. | n.a. | n.a. | n.a. | n.a. | n.a. | n.a. | n.a. | 1·02 | 1·07 | 1·19 | 0·18 | 0·04 | 0·25 | n.a. |
| Dy | 4·24 | 4·06 | 4·00 | 3·92 | 5·02 | 4·17 | 6·48 | 3·37 | 4·15 | 5·45 | 5·20 | 5·13 | 4·37 | 5·04 | 5·69 | 5·86 | 6·50 | 1·27 | 0·29 | 1·74 | 4·82 |
| Ho | n.a. | n.a. | n.a. | n.a. | n.a. | n.a. | n.a. | n.a. | n.a. | n.a. | n.a. | n.a. | n.a. | n.a. | 1·13 | 1·17 | 1·22 | 0·25 | 0·06 | 0·37 | n.a. |
| Er | 2·47 | 2·05 | 2·18 | 2·15 | 2·70 | 2·01 | 3·32 | 1·72 | 1·89 | 3·01 | 2·56 | 2·65 | 2·21 | 2·91 | 2·48 | 2·67 | 2·88 | 0·79 | 0·17 | 0·95 | 2·70 |
| Tm | n.a. | n.a. | n.a. | n.a. | n.a. | n.a. | n.a. | n.a. | n.a. | n.a. | n.a. | n.a. | n.a. | n.a. | 0·42 | 0·40 | 0·46 | 0·14 | 0·04 | 0·17 | n.a. |
| Yb | 2·87 | 1·95 | 2·53 | 2·55 | 3·20 | 2·09 | 3·62 | 1·98 | 1·86 | 3·61 | 2·30 | 2·46 | 1·79 | 2·99 | 2·32 | 2·37 | 2·71 | 1·02 | 0·28 | 1·10 | 2·87 |
| Lu | 0·42 | 0·29 | 0·41 | 0·36 | 0·49 | 0·31 | 0·51 | 0·28 | 0·28 | 0·50 | 0·39 | 0·43 | 0·33 | 0·42 | 0·40 | 0·38 | 0·44 | 0·17 | 0·05 | 0·15 | 0·52 |
| Eu/Eu* | 0·96 | 0·67 | 0·84 | 0·71 | 0·86 | 0·76 | 0·62 | 0·74 | 0·70 | 0·81 | 0·57 | 0·54 | 0·65 | 0·76 | 0·53 | 0·56 | 0·52 | 4·17 | 16·31 | 3·16 | 0·58 |
| (La/Yb)$n$ | 6·5 | 14·1 | 9·6 | 12·9 | 8·0 | 14·1 | 9·7 | 12·3 | 16·5 | 9·2 | 11·3 | 11·4 | 16·4 | 7·4 | 11·9 | 11·8 | 12·9 | 3·1 | 4·2 | 2·6 | 10·1 |
| Y | 31 | 27 | 31 | 31 | 37 | 26 | 47 | 23 | 28 | 44 | 34 | 32 | 27 | 35 | 28 | 31 | 31 | 8 | 2 | 11 | 27 |
| Zr | 229 | 249 | 198 | 167 | 217 | 242 | 391 | 216 | 185 | 171 | 229 | 242 | 242 | 188 | 266 | 270 | 304 | 56 | 38 | 41 | 216 |
| Hf | n.a. | n.a. | n.a. | n.a. | n.a. | n.a. | n.a. | n.a. | n.a. | n.a. | n.a. | n.a. | n.a. | n.a. | n.a. | n.a. | n.a. | n.a. | 1·0 | 1·0 | n.a. |
| Th | n.a. | n.a. | n.a. | n.a. | n.a. | n.a. | n.a. | n.a. | n.a. | n.a. | n.a. | n.a. | n.a. | n.a. | n.a. | n.a. | n.a. | n.a. | 0·3 | 1·1 | 13 |
| U | n.a. | n.a. | n.a. | n.a. | n.a. | n.a. | n.a. | n.a. | n.a. | n.a. | n.a. | n.a. | n.a. | n.a. | n.a. | n.a. | n.a. | n.a. | 3·2 | 2·6 | n.a. |
| V | 140 | 163 | 109 | 109 | 149 | 116 | 124 | 128 | 101 | 125 | 80 | 84 | 83 | 79 | 71 | 61 | 80 | 2·4 | 2·4 | 2·5 | n.a. |
| Nb | 12 | 12 | 11 | 13 | 13 | 16 | 36 | 14 | 16 | 15 | 14 | 11 | 12 | 11 | 13 | 12 | 15 | 1·6 | 0·8 | 1·2 | 13 |
| Cr | n.a. | n.a. | n.a. | n.a. | n.a. | n.a. | n.a. | n.a. | n.a. | n.a. | n.a. | n.a. | n.a. | n.a. | 45 | 43 | 53 | 4·3 | 5·1 | 2·8 | n.a. |
| Co | 73 | 42 | 30 | 31 | 33 | 26 | 40 | 40 | 32 | 42 | 11 | 19 | 15 | 11 | 39 | 36 | 53 | 82 | 76 | 84 | n.a. |
| Ni | 89 | 105 | 40 | 41 | 61 | 42 | 56 | 56 | 46 | 53 | 34 | 35 | 42 | 40 | 22 | 19 | 22 | 2 | 3 | 2 | 43 |
| Mg# | 37 | 39 | 42 | 39 | 44 | 38 | 41 | 39 | 40 | 42 | 40 | 38 | 44 | 36 | 37 | 39 | 37 | 35 | 21 | 45 | 38 |
| Rb/Sr | 0·81 | 0·95 | 0·91 | 0·86 | 0·94 | 0·75 | 0·90 | 1·07 | 0·86 | 1·21 | 0·76 | 1·10 | 0·40 | 1·03 | 1·75 | 1·76 | 1·22 | 1·22 | 0·62 | 0·71 | 0·91 |
| Sr/Ba | 0·32 | 0·23 | 0·32 | 0·40 | 0·25 | 0·33 | 0·28 | 0·24 | 0·29 | 0·23 | 0·29 | 0·27 | 0·92 | 0·19 | 0·21 | 0·17 | 0·18 | 0·25 | 0·26 | 0·31 | 0·29 |
| Rb/Zr | 0·44 | 0·50 | 0·91 | 1·03 | 0·61 | 0·52 | 0·37 | 0·66 | 0·94 | 1·08 | 0·57 | 0·67 | 0·58 | 0·70 | 0·73 | 0·79 | 0·58 | 2·34 | 4·30 | 3·36 | 0·75 |
| Ti/Nb | 420 | 480 | 327 | 295 | 392 | 304 | 125 | 347 | 281 | 316 | 330 | 425 | 440 | 425 | 322 | 355 | 347 | 154 | 146 | 207 | 395 |
| Sm/Nd | 0·237 | 0·213 | 0·226 | 0·230 | 0·238 | 0·211 | 0·230 | 0·213 | 0·217 | 0·229 | 0·229 | 0·215 | 0·201 | 0·220 | 0·214 | 0·209 | 0·201 | 0·237 | 0·240 | 0·280 | 0·226 |

NB: Nebulites; LG: Leucogranites. Data as in Table 2. n.a.: not analysed.
Layos (avg.): from data in Barbero & Villaseca (1992) and Barbero *et al.* (1995).

The other two samples in Table 4 have relatively high abundances of HREE, Y, V, Cr, Ni, Cu and negative Ce anomalies. Samples SSA-7 and SSA-8 have major element compositions comparable to those of the common sedimentary rocks in Table 2, but lower concentrations of Sr, Cs, V, Cr, Ni, Co, Cu, low Eu/Eu* and high Ce/Ce* ratios. However, samples SSA-7 and SSA-8 are not homogeneous and show varying abundances of Be, Sr, REE, Y and Nb apparently unrelated to the effects of major element dilution and varying ratios of Eu/Eu*, Sm/Nd and $(La/Yb)_n$. Except for the cordieritites, all rocks in Table 4 are samples from sedimentary units close to or above the Upper Neoproterozoic/Lower Cambrian unconformity. The low concentrations of the transition metals V, Cr, Ni, Cu (and to a lesser extent Co) in detrital rocks are consistent with significant changes in the geochemical environment of sedimentation.

The relatively high $P_2O_5$ of the cordieritites (1·1–3·8%) is reflected in abundant equant and euhedral crystals of apatite included in quartz, plagioclase, biotite and cordierite. Apatite thus appears to predate all major metamorphic phases suggesting the possibility of relatively high concentrations of primary phosphates in some sedimentary rocks (or possibly their precipitation during diagenesis).

**4.1.3. Granites.** Analytical data for the amphible-bearing, biotite and cordierite-bearing biotite granites are given in Table 5 along with analyses for the two mica granite types in Table 6. Ugidos & Recio (1993) published mean analyses for the main rock types and concluded that the amphibole-bearing and biotite granites probably derived from the same or similar protoliths of hybrid composition, as is suggested by their geochemical affinities (major oxides, trace elements, REE) and fractionation trends in binary variation diagrams. Despite significant mineralogical differences, probably related to differences in residual mineralogy entrained in these two granites, the geochemical data indicate tight evolutionary trends in several variation diagrams involving the amphibole-bearing, biotite, and the cordierite-bearing biotite granites (both internal and marginal). The REE contents and patterns of the biotite granites, internal and marginal cordierite-bearing granites, nebulites and shales show no major differences, and the degree of REE fractionation is moderate for all these rocks. The present study makes use of more comprehensive chemical data, including a suite of new whole rock Sr–Nd isotopic data to evaluate this model.

CaO and Eu/Eu* ratios are important to the petrogenetic discussions. The amphibole-bearing and biotite granites have overlapping CaO contents (2·6–3·8% and 1·9–3·2%, respectively) and Eu/Eu* ratios (0·55–0·83 and 0·38–0·76), whereas internal and marginal cordierite-bearing granites have rather lower CaO contents (1·7–2·9% and 1·3–2·3%) and Eu/Eu* ratios (0·34–0·65; 0·41–0·64) that partially overlap those of amphibole-bearing and biotite granites. The Bañobarez-Villavieja granites have CaO contents (0·44–1·5%) and Eu/Eu* ratios (0·24–0·44) that partially overlap those of marginal cordierite-bearing granites. All these granites have higher CaO contents and/or lower Eu/Eu* ratios than the shales, sandstones and nebulites. Bohoyo and Navalonguilla granites have similar CaO contents to some shales and sandstones but lower Eu/Eu* ratios (0·26–0·46), and El Payo granite samples overlap the CaO contents of nebulites with lower Eu/Eu* ratios (0·32–0·47). Only the biotite granites and internal cordierite-bearing biotite granites show any significant CaO–Eu/Eu* correlation (r=0·77 and 0·91, respectively; both >99% confidence level).

Calculations of zircon saturation temperatures from whole rock Zr and major oxide compositions (Watson & Harrison 1983) indicate temperatures of 794°C ± 18 for amphibole-bearing biotite granites, 807°C ± 36 for biotite granites, and 796°C ± 22 and 792°C ± 34 for internal and marginal cordierite-bearing biotite granites, respectively (all 2s). Back-scattered electron imaging studies indicate considerable zircon inheritance in the cordierite granites and the substantial overlap in the results is probably due to all facies being oversaturated in zircon, rather than reflecting magmatic equilibrium temperatures. Apatite-saturation temperatures calculated using a method appropriate for metaluminous to slightly peraluminous systems (Harrison & Watson 1984) indicate temperatures of 952°C ± 30 for amphibole-bearing, 976°C ± 28 for

**Table 4** Analyses of cordieritites and heterogeneous Lower Cambrian rocks S of Salamanca (Central Iberian Zone).

| Sample | CORD-1 | CORD-2 | SSA-7 | SSA-8 | PHA-1 | PHA-2 |
|---|---|---|---|---|---|---|
| $SiO_2$ | 47·17 | 51·03 | 73·33 | 61·75 | 67·74 | 40·44 |
| $TiO_2$ | b.d. | 0·32 | 0·60 | 0·88 | 0·27 | 0·33 |
| $Al_2O_3$ | 26·20 | 19·95 | 12·47 | 18·10 | 5·10 | 11·25 |
| $Fe_2O_3$ | 9·21 | 6·50 | 4·31 | 6·47 | 5·65 | 3·96 |
| MnO | 0·32 | 0·44 | 0·05 | 0·08 | 0·11 | b.d. |
| MgO | 4·17 | 2·36 | 1·59 | 2·90 | 0·16 | 1·28 |
| CaO | 1·94 | 6·80 | 1·12 | 0·60 | 9·54 | 19·23 |
| $Na_2O$ | 0·40 | 1·14 | 2·71 | 1·68 | 0·72 | 0·50 |
| $K_2O$ | 3·81 | 3·66 | 1·74 | 3·48 | 0·83 | 2·15 |
| $P_2O_5$ | 1·14 | 3·84 | 0·10 | 0·22 | 6·83 | 13·93 |
| LOI | 5·36 | 3·71 | 1·78 | 3·56 | 2·58 | 6·65 |
| total | 99·74 | 99·74 | 99·80 | 99·72 | 99·53 | 99·72 |
| Rb | 241 | 346 | 221 | 132 | 33 | 75 |
| Cs | 16 | 53 | 1·1 | 1·7 | 2·3 | 4·1 |
| Be | 750 | 815 | 9·2 | 1·5 | 1·8 | 2·1 |
| Sr | 11 | 33 | 8 | 53 | 322 | 349 |
| Ba | 80 | 117 | 89 | 465 | 176 | 394 |
| La | 16·0 | 85·6 | 21·0 | 77·7 | 41·6 | 134 |
| Ce | 44·2 | 224·6 | 69·4 | 159·7 | 91·7 | 253 |
| Pr | 6·55 | 30·8 | 7·02 | 16·1 | 12·8 | 31·8 |
| Nd | 28·4 | 127 | 26·8 | 58·2 | 58·5 | 133 |
| Sm | 9·61 | 33·5 | 9·29 | 10·3 | 20·4 | 36·1 |
| Eu | 0·30 | 2·17 | 0·06 | 0·95 | 6·46 | 9·35 |
| Gd | 10·5 | 30·9 | 8·68 | 7·32 | 23·0 | 54·5 |
| Tb | 1·94 | 5·47 | 1·98 | 1·10 | 3·11 | 10·8 |
| Dy | 12·8 | 31·3 | 13·1 | 5·81 | 16·3 | 73·3 |
| Ho | 2·36 | 5·70 | 2·85 | 1·21 | 3·09 | 16·4 |
| Er | 6·17 | 14·8 | 7·54 | 3·15 | 7·01 | 38·2 |
| Tm | 0·99 | 2·26 | 1·27 | 0·49 | 1·04 | 5·26 |
| Yb | 5·91 | 14·22 | 7·5 | 2·95 | 6·17 | 29·1 |
| Lu | 0·75 | 2·16 | 1·14 | 0·45 | 0·92 | 3·66 |
| Eu/Eu* | 0·09 | 0·21 | 0·02 | 0·33 | 0·91 | 0·64 |
| (La/Yb)*n* | 1·8 | 4·1 | 1·9 | 17·8 | 4·6 | 3·1 |
| Y | 73 | 174 | 72 | 30 | 101 | 447 |
| Zr | 87 | 324 | 302 | 364 | 31 | 9 |
| Th | 2·8 | 14 | 28 | 14 | 26 | 11 |
| U | 4·5 | 22 | 6·5 | 2·6 | 15 | 5·2 |
| V | 3 | 19 | b.d. | 12 | 36 | 75 |
| Nb | 2 | 17 | 31 | 13 | 6 | 10 |
| Cr | b.d. | 23 | 5 | 4 | 169 | 134 |
| Co | 18 | 22 | b.d. | 2 | 15 | 6 |
| Ni | b.d. | 10 | 5 | 2 | 26 | 18 |
| Mg# | 47 | 42 | 42 | 47 | 5 | 39 |
| Ce/Ce* | 1·01 | 1·02 | 1·34 | 1·06 | 0·93 | 0·91 |
| Sm/Nd | 0·338 | 0·263 | 0·347 | 0·177 | 0·349 | 0·271 |

CORD: Cordieritites; SSA: Altered rocks; PHA: Phosphorous-rich rocks.
Data as in Table 1; b.d.: below detection limit.

https://doi.org/10.1017/S1755691009008159 Published online by Cambridge University Press

**Table 5** Analyses of late Variscan granites S and SE of Salamanca (Central Iberian Zone).

| Sample | AG MIRA-1 | AG MIRA-2 | AG MIRA-3 | AG MIRA-4 | AG CARA-1 | AG CARA-2 | AG CARA-3 | AG CARA-4 | AG CARA-5 | AG CARA-6 | AG CARA-7 | AG CARA-8 | BG CARA-9 | BG MIRA-5 | BG VAA-1 | BG VAA-2 | BG VAA-3 | BG VAA-5 | BG VAA-7 | BG VAA-8 | BG VAA-11 | BG CARA-11 | CARA-15 |
|---|---|---|---|---|---|---|---|---|---|---|---|---|---|---|---|---|---|---|---|---|---|---|---|
| $SiO_2$ | 62·80 | 63·07 | 62·22 | 64·30 | 66·84 | 67·96 | 67·25 | 65·70 | 67·20 | 68·13 | 67·49 | 68·14 | 67·57 | 66·46 | 65·42 | 68·26 | 69·72 | 64·91 | 64·54 | 63·71 | 64·62 | 67·24 | 70·34 |
| $TiO_2$ | 0·80 | 0·86 | 0·79 | 0·73 | 0·54 | 0·52 | 0·57 | 0·64 | 0·57 | 0·49 | 0·52 | 0·54 | 0·49 | 0·69 | 0·66 | 0·63 | 0·57 | 0·79 | 0·72 | 0·85 | 0·65 | 0·48 | 0·35 |
| $Al_2O_3$ | 16·40 | 16·42 | 16·78 | 16·02 | 15·08 | 14·96 | 15·40 | 15·53 | 15·39 | 14·99 | 15·22 | 15·24 | 14·97 | 15·82 | 15·55 | 14·90 | 14·59 | 15·71 | 15·63 | 16·03 | 16·35 | 15·23 | 14·21 |
| $Fe_2O_3$ | 5·23 | 5·36 | 5·21 | 4·73 | 3·72 | 3·59 | 3·80 | 4·05 | 4·04 | 3·34 | 3·56 | 3·60 | 3·44 | 4·47 | 4·27 | 3·66 | 3·51 | 4·73 | 4·93 | 5·46 | 4·65 | 3·54 | 2·86 |
| MnO | 0·07 | 0·08 | 0·08 | 0·07 | 0·06 | 0·06 | 0·07 | 0·06 | 0·06 | 0·06 | 0·06 | 0·06 | 0·06 | 0·06 | 0·06 | 0·06 | 0·07 | 0·06 | 0·06 | 0·07 | 0·60 | 0·05 | 0·05 |
| MgO | 1·89 | 1·97 | 1·96 | 1·58 | 1·23 | 1·27 | 1·38 | 1·53 | 1·53 | 1·28 | 1·29 | 1·34 | 1·23 | 1·31 | 1·24 | 1·06 | 0·99 | 1·32 | 1·35 | 1·58 | 1·60 | 1·33 | 0·96 |
| CaO | 3·84 | 3·79 | 3·82 | 3·41 | 2·77 | 2·58 | 2·91 | 3·11 | 2·92 | 2·78 | 2·62 | 2·64 | 2·63 | 2·84 | 2·63 | 2·42 | 2·26 | 2·82 | 2·59 | 3·22 | 3·17 | 2·56 | 1·91 |
| $Na_2O$ | 3·57 | 3·55 | 3·68 | 3·54 | 3·49 | 3·36 | 3·47 | 3·46 | 3·47 | 3·50 | 3·47 | 3·44 | 3·43 | 3·48 | 3·45 | 3·46 | 3·46 | 3·31 | 3·50 | 3·49 | 3·54 | 3·37 | 3·29 |
| $K_2O$ | 3·35 | 3·46 | 3·50 | 3·75 | 3·94 | 4·18 | 3·84 | 3·88 | 3·89 | 3·97 | 4·02 | 4·05 | 4·02 | 4·22 | 4·36 | 4·18 | 4·10 | 4·52 | 4·12 | 3·90 | 3·95 | 4·16 | 4·44 |
| $P_2O_5$ | 0·28 | 0·27 | 0·28 | 0·25 | 0·17 | 0·19 | 0·21 | 0·23 | 0·22 | 0·21 | 0·26 | 0·20 | 0·19 | 0·29 | 0·28 | 0·21 | 0·20 | 0·27 | 0·38 | 0·31 | 0·28 | 0·24 | 0·20 |
| LOI | 0·68 | 0·81 | 0·78 | 0·76 | 0·73 | 0·68 | 0·64 | 0·67 | 0·62 | 0·66 | 0·70 | 0·71 | 0·77 | 0·82 | 0·73 | 0·79 | 1·01 | 0·92 | 0·82 | 0·80 | 0·60 | 1·00 | 1·01 |
| total | 98·91 | 99·64 | 99·10 | 99·14 | 98·57 | 99·35 | 99·54 | 99·96 | 99·91 | 99·41 | 99·21 | 99·96 | 98·80 | 100·5 | 98·65 | 99·63 | 100·5 | 99·36 | 98·66 | 99·42 | 99·47 | 99·2 | 99·62 |
| Rb | 136 | 143 | 145 | 154 | 164 | 178 | 163 | 146 | 148 | 165 | 160 | 168 | 166 | 168 | 189 | 196 | 206 | 175 | 206 | 165 | 155 | 165 | 195 |
| Sr | 218 | 217 | 204 | 168 | 158 | 148 | 165 | 177 | 159 | 144 | 147 | 157 | 156 | 167 | 162 | 137 | 126 | 190 | 141 | 198 | 195 | 152 | 105 |
| Ba | 683 | 652 | 601 | 605 | 483 | 511 | 523 | 584 | 540 | 757 | 516 | 528 | 712 | 650 | 598 | 454 | 383 | 778 | 532 | 722 | 666 | 530 | 416 |
| ASI | 1·04 | 1·04 | 1·04 | 1·03 | 1·03 | 1·05 | 1·05 | 1·03 | 1·05 | 1·02 | 1·07 | 1·06 | 1·04 | 1·07 | 1·07 | 1·05 | 1·06 | 1·06 | 1·11 | 1·06 | 1·07 | 1·08 | 1·07 |
| La | 34·6 | 37·3 | 45·5 | 37·1 | 30·9 | 25·6 | 27·8 | 38·7 | 19·3 | 24·4 | 26·8 | 27·4 | 23·1 | 39·7 | 37·6 | 33·5 | 33·6 | 46·6 | 44·9 | 53·8 | 36·2 | 27·7 | 24·1 |
| Ce | 74·3 | 78·9 | 93·8 | 76·8 | 66·4 | 55·4 | 59·9 | 81·2 | 42·4 | 55·5 | 59·0 | 60·6 | 52·2 | 84·6 | 81·6 | 72·3 | 74·3 | 97·3 | 97·1 | 105 | 75·0 | 59·0 | 52·6 |
| Pr | n.a. | n.a. | n.a. | n.a. | n.a. | n.a. | n.a. | n.a. | n.a. | n.a. | n.a. | n.a. | n.a. | n.a. | n.a. | n.a. | n.a. | n.a. | n.a. | n.a. | n.a. | n.a. | n.a. |
| Nd | 30·6 | 32·7 | 37·8 | 31·0 | 25·7 | 23·7 | 25·8 | 33·0 | 20·6 | 23·8 | 26·5 | 26·7 | 23·0 | 35·5 | 33·8 | 30·7 | 31·6 | 38·2 | 38·2 | 41·6 | 34·4 | 26·5 | 22·9 |
| Sm | 6·87 | 7·45 | 7·86 | 6·68 | 6·02 | 5·56 | 6·17 | 7·09 | 5·40 | 5·62 | 6·04 | 6·12 | 5·42 | 7·75 | 7·30 | 7·09 | 7·22 | 7·41 | 8·98 | 8·73 | 7·51 | 6·03 | 5·72 |
| Eu | 1·51 | 1·76 | 1·33 | 1·33 | 1·34 | 0·97 | 1·04 | 1·24 | 0·88 | 0·95 | 0·96 | 0·98 | 1·14 | 1·43 | 0·89 | 1·08 | 0·82 | 1·51 | 1·36 | 1·78 | 1·22 | 0·91 | 0·65 |
| Gd | 5·13 | 5·63 | 5·64 | 4·86 | 4·31 | 4·14 | 4·72 | 4·98 | 4·35 | 4·61 | 4·77 | 4·55 | 4·14 | 5·62 | 5·37 | 5·32 | 5·37 | 4·96 | 6·66 | 6·16 | 6·00 | 4·82 | 4·72 |
| Tb | n.a. | n.a. | n.a. | n.a. | n.a. | n.a. | n.a. | n.a. | n.a. | n.a. | n.a. | n.a. | n.a. | n.a. | n.a. | n.a. | n.a. | n.a. | n.a. | n.a. | n.a. | n.a. | n.a. |
| Dy | 4·36 | 5·26 | 4·77 | 4·18 | 3·92 | 3·88 | 4·53 | 4·22 | 4·41 | 4·50 | 4·35 | 4·45 | 3·96 | 4·72 | 4·54 | 4·81 | 5·09 | 3·48 | 7·94 | 4·65 | 4·85 | 4·26 | 4·49 |
| Ho | n.a. | n.a. | n.a. | n.a. | n.a. | n.a. | n.a. | n.a. | n.a. | n.a. | n.a. | n.a. | n.a. | n.a. | n.a. | n.a. | n.a. | n.a. | n.a. | n.a. | n.a. | n.a. | n.a. |
| Er | 2·19 | 2·79 | 2·22 | 2·08 | 2·07 | 2·04 | 2·45 | 2·15 | 2·33 | 2·39 | 2·29 | 2·29 | 2·06 | 2·30 | 2·22 | 2·45 | 2·54 | 1·47 | 3·86 | 2·23 | 2·44 | 2·27 | 2·52 |
| Tm | n.a. | n.a. | n.a. | n.a. | n.a. | n.a. | n.a. | n.a. | n.a. | n.a. | n.a. | n.a. | n.a. | n.a. | n.a. | n.a. | n.a. | n.a. | n.a. | n.a. | n.a. | n.a. | n.a. |
| Yb | 2·14 | 3·32 | 2·15 | 2·16 | 2·31 | 2·27 | 2·95 | 2·34 | 2·66 | 2·78 | 2·48 | 2·54 | 2·37 | 2·29 | 2·27 | 2·68 | 2·83 | 1·48 | 5·37 | 2·27 | 2·16 | 2·23 | 2·62 |
| Lu | 0·3 | 0·48 | 0·32 | 0·31 | 0·32 | 0·33 | 0·43 | 0·30 | 0·34 | 0·33 | 0·31 | 0·35 | 0·31 | 0·31 | 0·32 | 0·38 | 0·36 | 0·23 | 0·64 | 0·33 | 0·38 | 0·39 | 0·40 |
| Eu/Eu* | 0·78 | 0·83 | 0·61 | 0·71 | 0·80 | 0·62 | 0·59 | 0·64 | 0·55 | 0·57 | 0·55 | 0·57 | 0·74 | 0·66 | 0·43 | 0·54 | 0·40 | 0·76 | 0·54 | 0·74 | 0·56 | 0·52 | 0·38 |
| (La/Yb)*n* | 11 | 7·6 | 14 | 12 | 9·0 | 7·6 | 6·4 | 11 | 4·9 | 5·9 | 7·3 | 7·3 | 6·6 | 12 | 11 | 8·5 | 8·0 | 21 | 5·7 | 16 | 11 | 8·4 | 6·2 |
| Y | 29 | 37 | 31 | 28 | 28 | 27 | 33 | 28 | 31 | 32 | 29 | 31 | 28 | 31 | 30 | 33 | 35 | 20 | 57 | 33 | 30 | 29 | 33 |
| Th | n.a. | n.a. | n.a. | n.a. | n.a. | n.a. | n.a. | n.a. | n.a. | n.a. | n.a. | n.a. | n.a. | n.a. | n.a. | n.a. | n.a. | n.a. | n.a. | n.a. | 11 | 12 | b.d. |
| Zr | 269 | 226 | 269 | 226 | 182 | 180 | 204 | 203 | 211 | 181 | 184 | 191 | 168 | 245 | 261 | 228 | 203 | 311 | 298 | 314 | 230 | 179 | 150 |
| Nb | 14 | 14 | 14 | 13 | 11 | 12 | 13 | 13 | 13 | 12 | 12 | 13 | 11 | 15 | 15 | 13 | 13 | 16 | 22 | 19 | 13 | 10 | 11 |
| V | 87 | 92 | 84 | 81 | 65 | 55 | 73 | 70 | 64 | 51 | 53 | 61 | 65 | 71 | 75 | 60 | 51 | 68 | 59 | 80 | 53 | 38 | 27 |
| Ni | 29 | 34 | 16 | 22 | 17 | 17 | 15 | 28 | 30 | 30 | 34 | 17 | 15 | 18 | 20 | b.d. | b.d. | 14 | 20 | 24 | 18 | 15 | 20 |
| Co | 25 | 28 | 41 | 37 | 22 | 29 | 22 | 31 | 43 | 33 | 37 | 30 | 20 | 33 | 29 | 15 | 17 | 19 | 22 | 43 | 7 | 7 | 7 |

Table 5 (continued)

| Sample | BG BEU-12 | BG BEU-13 | ICG XSA-4 | ICG XSA-5 | ICG XSA-7 | ICG XSA-8 | ICG BEU-14 | ICG BEU-15 | ICG BEU-16 | ICG BEU-17 | ICG GU-12 | ICG PHU-1 | MCG XSA-6 | MCG XSA-9 | MCG XSA-10 | MCG XSA-11 | MCG MC-9 | MCG SEU-5 | MCG SEU-6 | MCG MC-10 | MCG MC-12 | MCG MC-13 | MCG SEU-7 | MCG MC-11 |
|---|---|---|---|---|---|---|---|---|---|---|---|---|---|---|---|---|---|---|---|---|---|---|---|---|
| $SiO_2$ | 68·2 | 67·21 | 66·14 | 67·93 | 65·02 | 69·04 | 69·68 | 64·68 | 68·42 | 65·29 | 67·59 | 70·31 | 69·2 | 68·69 | 68·45 | 68·42 | 69·64 | 69·77 | 68·54 | 66·42 | 65·95 | 69·17 | 66·93 | 68·29 |
| $TiO_2$ | 0·44 | 0·48 | 0·54 | 0·56 | 0·64 | 0·48 | 0·40 | 0·64 | 0·44 | 0·64 | 0·52 | 0·38 | 0·43 | 0·44 | 0·56 | 0·44 | 0·34 | 0·40 | 0·45 | 0·56 | 0·56 | 0·39 | 0·54 | 0·52 |
| $Al_2O_3$ | 15·03 | 15·18 | 15·73 | 15·26 | 16·78 | 14·75 | 14·58 | 16·32 | 15·30 | 15·83 | 15·75 | 14·56 | 15·21 | 15·57 | 15·16 | 15·33 | 15·26 | 15·03 | 15·42 | 16·25 | 15·78 | 15·66 | 15·81 | 15·43 |
| $Fe_2O_3$ | 3·34 | 3·50 | 3·84 | 4·00 | 4·50 | 3·45 | 3·12 | 4·41 | 3·22 | 4·58 | 3·90 | 3·00 | 3·08 | 3·27 | 3·74 | 3·02 | 2·75 | 2·90 | 3·32 | 4·01 | 4·09 | 2·77 | 3·95 | 3·84 |
| MnO | 0·05 | 0·05 | 0·05 | 0·03 | 0·05 | 0·04 | 0·04 | 0·06 | 0·05 | 0·06 | 0·05 | 0·05 | 0·05 | 0·05 | 0·05 | 0·05 | 0·05 | 0·05 | 0·05 | 0·06 | 0·06 | 0·04 | 0·06 | 0·06 |
| MgO | 0·93 | 1·03 | 1·20 | 1·25 | 1·38 | 1·08 | 0·64 | 1·35 | 1·03 | 1·45 | 0·85 | 0·81 | 1·04 | 1·04 | 1·18 | 0·93 | 0·53 | 0·91 | 1·03 | 1·01 | 1·00 | 0·80 | 1·11 | 0·96 |
| CaO | 2·08 | 2·29 | 2·47 | 2·50 | 3·02 | 2·06 | 1·70 | 2·62 | 1·91 | 2·87 | 2·12 | 1·70 | 2·25 | 1·70 | 2·07 | 1·67 | 1·45 | 1·75 | 1·97 | 1·70 | 1·70 | 1·53 | 1·82 | 1·67 |
| $Na_2O$ | 3·27 | 3·40 | 3·50 | 3·27 | 3·59 | 3·27 | 3·17 | 3·40 | 3·22 | 3·47 | 3·37 | 3·34 | 3·52 | 3·27 | 3·16 | 3·32 | 3·33 | 3·37 | 3·40 | 3·27 | 3·24 | 3·45 | 3·37 | 3·29 |
| $K_2O$ | 4·57 | 4·41 | 4·66 | 4·58 | 4·19 | 4·57 | 4·48 | 4·30 | 4·39 | 3·83 | 4·34 | 4·37 | 4·14 | 4·59 | 4·08 | 4·37 | 4·50 | 4·33 | 4·49 | 4·75 | 4·44 | 4·50 | 4·73 | 4·44 |
| $P_2O_5$ | 0·25 | 0·26 | 0·30 | 0·30 | 0·30 | 0·29 | 0·19 | 0·34 | 0·24 | 0·32 | 0·27 | 0·24 | 0·32 | 0·39 | 0·40 | 0·39 | 0·26 | 0·27 | 0·34 | 0·32 | 0·32 | 0·34 | 0·38 | 0·34 |
| LOI | 1·04 | 0·81 | 0·80 | 0·55 | 0·81 | 0·72 | 0·76 | 0·93 | 1·16 | 0·91 | 0·96 | 0·59 | 0·60 | 0·76 | 0·88 | 0·86 | 0·91 | 0·78 | 0·68 | 1·18 | 1·36 | 1·12 | 1·04 | 0·73 |
| total | 99·2 | 98·62 | 99·23 | 100·2 | 100·3 | 99·75 | 98·76 | 99·05 | 99·18 | 99·25 | 99·72 | 99·35 | 99·84 | 99·75 | 99·73 | 98·8 | 99·02 | 99·56 | 99·69 | 99·53 | 98·5 | 99·77 | 99·74 | 99·57 |
| Rb | 194 | 192 | 191 | 169 | 159 | 206 | 180 | 196 | 200 | 166 | 195 | 212 | 192 | 277 | 230 | 281 | 236 | 234 | 242 | 233 | 231 | 275 | 234 | 242 |
| Sr | 140 | 143 | 157 | 147 | 209 | 132 | 82 | 174 | 131 | 178 | 114 | 106 | 205 | 151 | 175 | 165 | 129 | 168 | 170 | 154 | 138 | 171 | 150 | 134 |
| Ba | 558 | 550 | 590 | 507 | 937 | 492 | 396 | 683 | 487 | 642 | 554 | 366 | 560 | 442 | 458 | 411 | 444 | 444 | 467 | 635 | 574 | 443 | 582 | 542 |
| ASI | 1·11 | 1·09 | 1·08 | 1·08 | 1·10 | 1·10 | 1·15 | 1·15 | 1·18 | 1·10 | 1·17 | 1·14 | 1·12 | 1·24 | 1·22 | 1·24 | 1·23 | 1·18 | 1·16 | 1·26 | 1·26 | 1·25 | 1·21 | 1·24 |
| La | 41·0 | 38·5 | 35·8 | 33·7 | 36·9 | 37·4 | 33·9 | 30·1 | 34·3 | 35·3 | 37·1 | 23·2 | 29·3 | 28·7 | 33·0 | 27·6 | 25·9 | 22·9 | 32·6 | 37·1 | 38·9 | 24·9 | 32·0 | 33·0 |
| Ce | 78·5 | 80·2 | 77·3 | 71·5 | 78·7 | 80·6 | 73·7 | 64·9 | 69·1 | 78·6 | 76·4 | 50·5 | 63·0 | 63·0 | 72·8 | 58·6 | 55·5 | 50·4 | 70·5 | 79·5 | 84·2 | 54·3 | 69·0 | 70·0 |
| Pr | n.a. | n.a. | n.a. | n.a. | n.a. | n.a. | n.a. | n.a. | n.a. | n.a. | n.a. | n.a. | n.a. | n.a. | n.a. | n.a. | n.a. | n.a. | n.a. | n.a. | n.a. | n.a. | n.a. | n.a. |
| Nd | 34·0 | 34·1 | 32·2 | 30·5 | 32·6 | 34·5 | 31·8 | 29·5 | 29·8 | 32·2 | 33·7 | 21·5 | 27·8 | 27·8 | 31·9 | 26·3 | 24·3 | 22·0 | 31·1 | 35·5 | 37·6 | 24·1 | 31·9 | 32·0 |
| Sm | 7·35 | 7·60 | 6·81 | 6·50 | 6·71 | 7·66 | 8·02 | 6·76 | 6·66 | 6·83 | 7·31 | 5·11 | 5·80 | 6·01 | 6·75 | 5·49 | 5·02 | 4·88 | 6·69 | 7·89 | 8·34 | 5·29 | 7·13 | 7·12 |
| Eu | 1·03 | 1·00 | 1·02 | 1·00 | 1·28 | 0·87 | 0·81 | 1·14 | 0·88 | 1·13 | 1·06 | 0·67 | 0·87 | 0·78 | 0·88 | 0·74 | 0·78 | 0·70 | 0·89 | 1·09 | 1·04 | 0·71 | 0·95 | 0·96 |
| Gd | 5·42 | 5·85 | 5·19 | 4·94 | 5·34 | 5·59 | 6·43 | 5·56 | 4·96 | 5·37 | 5·77 | 3·88 | 4·35 | 4·20 | 4·66 | 3·88 | 3·99 | 3·72 | 4·78 | 6·24 | 6·26 | 3·97 | 5·78 | 5·87 |
| Tb | n.a. | n.a. | n.a. | n.a. | n.a. | n.a. | n.a. | n.a. | n.a. | n.a. | n.a. | n.a. | n.a. | n.a. | n.a. | n.a. | n.a. | n.a. | n.a. | n.a. | n.a. | n.a. | n.a. | n.a. |
| Dy | 4·24 | 4·88 | 4·46 | 4·00 | 3·85 | 4·49 | 6·78 | 4·17 | 4·16 | 4·25 | 4·72 | 3·70 | 3·37 | 3·12 | 3·45 | 2·95 | 2·96 | 3·08 | 3·54 | 5·24 | 5·18 | 3·02 | 4·83 | 5·02 |
| Ho | n.a. | n.a. | n.a. | n.a. | n.a. | n.a. | n.a. | n.a. | n.a. | n.a. | n.a. | n.a. | n.a. | n.a. | n.a. | n.a. | n.a. | n.a. | n.a. | n.a. | n.a. | n.a. | n.a. | n.a. |
| Er | 2·19 | 2·63 | 2·30 | 2·04 | 1·68 | 2·31 | 4·01 | 1·75 | 2·25 | 2·19 | 2·43 | 1·96 | 1·65 | 1·47 | 1·61 | 1·37 | 1·47 | 1·60 | 1·67 | 2·77 | 2·59 | 1·36 | 2·60 | 2·69 |
| Tm | n.a. | n.a. | n.a. | n.a. | n.a. | n.a. | n.a. | n.a. | n.a. | n.a. | n.a. | n.a. | n.a. | n.a. | n.a. | n.a. | n.a. | n.a. | n.a. | n.a. | n.a. | n.a. | n.a. | n.a. |
| Yb | 2·16 | 2·49 | 2·15 | 1·85 | 1·86 | 2·17 | 3·65 | 1·06 | 2·19 | 2·04 | 2·28 | 1·89 | 1·50 | 1·36 | 1·43 | 1·22 | 1·39 | 1·62 | 1·52 | 2·59 | 2·38 | 1·19 | 2·40 | 2·57 |
| Lu | 0·33 | 0·42 | 0·35 | 0·30 | 0·34 | 0·37 | 0·57 | 0·16 | 0·38 | 0·32 | 0·39 | 0·32 | 0·19 | 0·37 | 0·38 | 0·21 | 0·20 | 0·27 | 0·26 | 0·46 | 0·35 | 0·19 | 0·41 | 0·38 |
| Eu/Eu* | 0·50 | 0·46 | 0·52 | 0·54 | 0·65 | 0·41 | 0·34 | 0·57 | 0·47 | 0·57 | 0·50 | 0·46 | 0·53 | 0·47 | 0·48 | 0·49 | 0·53 | 0·50 | 0·48 | 0·47 | 0·44 | 0·47 | 0·45 | 0·45 |
| (La/Yb)*n* | 13 | 10 | 11 | 12 | 13 | 12 | 6·3 | 19 | 11 | 12 | 11 | 8·3 | 13 | 14 | 14 | 15 | 13 | 9·6 | 14 | 9·7 | 11 | 14 | 9·0 | 8·7 |
| Y | 30 | 34 | 29 | 26 | 22 | 29 | 52 | 24 | 30 | 28 | 31 | 25 | 21 | 19 | 21 | 18 | 19 | 20 | 21 | 35 | 33 | 18 | 31 | 34 |
| Th | 20 | 23 | 6 | b.d. | b.d. | 23 | 20 | 13 | 17 | 15 | b.d. | 14 | b.d. | 16 | 17 | 13 | b.d. | 11 | 17 | b.d. | 17 | b.d. | 15 | 15 |
| Zr | 189 | 181 | 187 | 185 | 223 | 199 | 165 | 202 | 171 | 232 | 202 | 135 | 169 | 159 | 185 | 152 | 138 | 133 | 157 | 226 | 224 | 126 | 198 | 184 |
| Nb | 13 | 14 | 14 | 12 | 12 | 10 | 13 | 13 | 12 | 12 | 12 | 9 | 11 | 11 | 11 | 12 | 8 | 9 | 14 | 7 | 16 | 10 | 14 | 14 |
| V | 33 | 30 | 45 | 42 | 10 | 8 | 34 | 48 | 30 | 45 | 40 | 30 | 25 | 27 | 36 | 26 | 11 | 10 | 27 | 14 | 35 | 21 | 38 | 38 |
| Ni | 6 | 12 | 20 | 14 | 19 | 76 | 7 | 6 | b.d. | 28 | 11 | 10 | 16 | b.d. | 8 | 14 | 5 | 9 | 17 | 10 | 11 | 6 | 18 | 18 |
| Co | 9 | 7 | 5 | b.d. | b.d. | 13 | 7 | 8 | 7 | 7 | 8 | 8 | b.d. | b.d. | b.d. | b.d. | 8 | 6 | 10 | 10 | 9 | b.d. | 10 | 10 |

AG: Amphibole-bearing biotite granites; BG: Biotite granites; ICG: Internal cordierite-bearing biotite granites; MCG: Marginal cordierite-bearing biotite granites. Data as in Table 2.
ASI: Alumina Saturation Index: $Al_2O_3/(Na_2O+K_2O+CaO^*)$ (molar); n.a.: not analysed; b.d.: below detection limit.

**Table 6** Analyses of cordierite-bearing two mica granites W and S of Salamanca (Central Iberian Zone).

| Sample | BVG VVA-2 | BVG VVA-7 | BVG VVA-11 | BVG VVA-27 | BVG CBH-5 | BVG CBH-10 | BVG CBH-15 | BVG CBH-38 | BVG CBH-46 | BVG CBH-54 | BohG I-11 | BohG I-15 | NavG BOA-1 | NavG BOA-2 | PayG FG-10 | PayG FG-11 | PayG GAT-4 |
|---|---|---|---|---|---|---|---|---|---|---|---|---|---|---|---|---|---|
| $SiO_2$ | 73·68 | 73·06 | 73·71 | 72·12 | 72·94 | 72·59 | 75·12 | 70·79 | 69·39 | 71·65 | 74·41 | 75·85 | 72·76 | 72·87 | 71·4 | 73·55 | 72·47 |
| $TiO_2$ | 0·11 | 0·17 | 0·20 | 0·25 | 0·14 | 0·17 | 0·16 | 0·39 | 0·48 | 0·34 | 0·26 | 0·23 | 0·13 | 0·10 | 0·31 | 0·16 | 0·27 |
| $Al_2O_3$ | 14·08 | 14·25 | 13·86 | 14·28 | 14·23 | 14·60 | 12·92 | 14·28 | 14·71 | 14·03 | 12·61 | 12·38 | 14·07 | 14·00 | 15·42 | 14·02 | 14·18 |
| $Fe_2O_3$ | 1·36 | 1·62 | 1·87 | 2·08 | 1·38 | 1·61 | 1·67 | 3·16 | 3·40 | 2·66 | 2·02 | 1·86 | 1·53 | 1·55 | 2·37 | 1·55 | 2·22 |
| MnO | 0·03 | 0·02 | 0·03 | 0·03 | 0·02 | 0·02 | 0·03 | 0·04 | 0·04 | 0·05 | 0·47 | 0·34 | 0·18 | 0·26 | 0·03 | b.d. | b.d. |
| MgO | 0·22 | 0·32 | 0·39 | 0·44 | 0·29 | 0·30 | 0·26 | 0·64 | 0·72 | 0·54 | 0·03 | 0·03 | 0·04 | 0·05 | 0·68 | 0·36 | 0·50 |
| CaO | 0·60 | 0·69 | 0·44 | 0·81 | 0·60 | 0·60 | 0·80 | 1·20 | 1·50 | 1·13 | 0·38 | 0·44 | 0·42 | 0·45 | 0·95 | 0·71 | 0·87 |
| $Na_2O$ | 3·54 | 3·52 | 2·97 | 3·27 | 3·40 | 3·59 | 3·29 | 3·25 | 3·40 | 3·33 | 3·05 | 3·16 | 3·39 | 3·43 | 3·07 | 3·27 | 2·68 |
| $K_2O$ | 4·98 | 5·08 | 4·94 | 5·23 | 5·58 | 5·25 | 4·75 | 5·08 | 5·33 | 5·12 | 4·35 | 3·75 | 5·09 | 4·78 | 5·04 | 4·67 | 5·49 |
| $P_2O_5$ | 0·29 | 0·3 | 0·25 | 0·25 | 0·34 | 0·30 | 0·10 | 0·22 | 0·24 | 0·22 | 0·25 | 0·31 | 0·25 | 0·27 | 0·30 | 0·30 | 0·21 |
| LOI | 0·71 | 0·70 | 1·10 | 0·68 | 0·71 | 0·75 | 0·69 | 0·70 | 0·52 | 0·57 | 1·07 | 0·72 | 0·82 | 0·76 | 0·81 | 1·18 | 0·89 |
| total | 99·6 | 99·73 | 99·76 | 99·44 | 99·63 | 99·78 | 99·79 | 99·75 | 99·73 | 99·64 | 98·9 | 99·07 | 98·68 | 98·52 | 100·38 | 99·77 | 99·78 |
| Rb | 368 | 352 | 335 | 299 | 352 | 359 | 282 | 277 | 268 | 288 | 269 | 280 | 338 | 307 | 291 | 358 | 263 |
| Cs | 39 | 29 | 27 | 29 | 24 | 31 | 16 | 18 | 17 | 22 | n.a. | n.a. | n.a. | n.a. | 21 | 19 | 13 |
| Be | 5·2 | 4·2 | 5·3 | 8·5 | 5·2 | 8·7 | 6·8 | 6·4 | 16 | 8·7 | n.a. | n.a. | n.a. | n.a. | 3·9 | 4·2 | 5·1 |
| Sr | 40 | 45 | 39 | 61 | 40 | 42 | 51 | 351 | 86 | 66 | 37 | 28 | 37 | 39 | 75 | 42 | 76 |
| Ba | 153 | 208 | 215 | 289 | 201 | 214 | 186 | 403 | 405 | 298 | 145 | 84 | 153 | 147 | 292 | 102 | 202 |
| ASI | 1·21 | 1·20 | 1·33 | 1·20 | 1·19 | 1·22 | 1·10 | 1·14 | 1·09 | 1·12 | 1·28 | 1·33 | 1·25 | 1·27 | 1·34 | 1·27 | 1·24 |
| La | 11·1 | 18·5 | 19·0 | 25·3 | 13·6 | 15·4 | 14·8 | 27·6 | 27·9 | 25·9 | 22·3 | 18·7 | 22·0 | 21·5 | 22·0 | 11·0 | 20·5 |
| Ce | 23·8 | 41·7 | 42·2 | 55·0 | 30·1 | 32·2 | 32·6 | 58·8 | 60·0 | 56·6 | 51·0 | 43·4 | 41·4 | 44·4 | 48·0 | 24·5 | 46·5 |
| Pr | 2·79 | 4·71 | 5·01 | 6·55 | 3·53 | 4·07 | 3·96 | 7·11 | 6·94 | 6·64 | n.a. | n.a. | n.a. | n.a. | 5·90 | 3·03 | 5·73 |
| Nd | 10·8 | 18·8 | 18·9 | 25·1 | 13·6 | 15·9 | 15·3 | 28·1 | 28·2 | 27·0 | 21·7 | 18·8 | 15·1 | 16·6 | 22·6 | 11·4 | 215 |
| Sm | 2·71 | 4·19 | 4·47 | 5·70 | 3·23 | 3·88 | 3·63 | 6·24 | 6·16 | 5·79 | 5·50 | 4·82 | 3·75 | 4·40 | 4·89 | 2·73 | 5·12 |
| Eu | 0·30 | 0·36 | 0·30 | 0·49 | 0·30 | 0·33 | 0·50 | 0·75 | 0·81 | 0·63 | 0·41 | 0·47 | 0·5 | 0·38 | 0·66 | 0·27 | 0·49 |
| Gd | 2·23 | 3·47 | 3·46 | 4·52 | 2·47 | 2·92 | 3·36 | 5·08 | 5·30 | 4·93 | 4·30 | 3·67 | 2·91 | 3·49 | 3·80 | 2·44 | 4·18 |
| Tb | 0·39 | 0·52 | 0·52 | 0·68 | 0·37 | 0·48 | 0·62 | 0·88 | 0·89 | 0·83 | n.a. | n.a. | n.a. | n.a. | 0·57 | 0·41 | 0·68 |
| Dy | 2·24 | 2·66 | 2·66 | 3·42 | 1·79 | 2·19 | 3·66 | 4·93 | 4·69 | 4·53 | 3·04 | 2·68 | 2·73 | 3·18 | 2·85 | 2·22 | 3·47 |
| Ho | 0·45 | 0·48 | 0·49 | 0·68 | 0·35 | 0·46 | 0·88 | 1·08 | 1·01 | 0·99 | n.a. | n.a. | n.a. | n.a. | 0·46 | 0·34 | 0·51 |
| Er | 0·91 | 1·08 | 1·14 | 1·53 | 0·81 | 0·99 | 2·24 | 2·62 | 2·40 | 2·38 | 1·24 | 1·14 | 1·21 | 1·51 | 1·13 | 0·79 | 1·13 |
| Tm | 0·14 | 0·17 | 0·18 | 0·22 | 0·12 | 0·17 | 0·39 | 0·41 | 0·41 | 0·38 | n.a. | n.a. | n.a. | n.a. | 0·15 | 0·11 | 0·14 |
| Yb | 1·00 | 1·06 | 1·16 | 1·62 | 0·80 | 1·08 | 2·83 | 2·94 | 2·81 | 2·55 | 1·20 | 1·10 | 1·28 | 1·58 | 0·99 | 0·69 | 0·82 |
| Lu | 0·12 | 0·15 | 0·16 | 0·22 | 0·11 | 0·14 | 0·43 | 0·41 | 0·38 | 0·38 | 0·15 | 0·15 | 0·17 | 0·26 | 0·14 | 0·09 | 0·11 |
| Eu/Eu* | 0·38 | 0·29 | 0·24 | 0·30 | 0·32 | 0·30 | 0·44 | 0·41 | 0·43 | 0·36 | 0·26 | 0·34 | 0·46 | 0·30 | 0·47 | 0·32 | 0·32 |
| (La/Yb)*n* | 7·5 | 12 | 11 | 11 | 11 | 9·7 | 3·6 | 6·3 | 6·7 | 6·9 | 13 | 12 | 12 | 9·2 | 15 | 11 | 17 |
| Y | 13 | 13 | 14 | 19 | 9 | 13 | 24 | 29 | 27 | 27 | 19 | 17 | 19 | 22 | 14 | 11 | 16 |
| Zr | 56 | 90 | 90 | 112 | 69 | 75 | 75 | 156 | 171 | 134 | 123 | 104 | 76 | 76 | 132 | 70 | 129 |
| Hf | 2·4 | 3·7 | 3·9 | 4·4 | 2·9 | 3·0 | 3·1 | 5·8 | 6·1 | 5·2 | n.a. | n.a. | n.a. | n.a. | 3·8 | 2·3 | 3·8 |
| Th | 7·8 | 12 | 13 | 19 | 8·4 | 10 | 12 | 16 | 15 | 16 | n.a. | n.a. | n.a. | n.a. | 12 | 8·0 | 16 |
| V | 5 | 8 | 9 | 13 | 5 | 6 | 9 | 22 | 30 | 20 | 29 | 31 | b.d. | 16 | 23 | 8 | 12 |
| Nb | 12 | 15 | 16 | 13 | 12 | 14 | 9 | 13 | 13 | 14 | 17 | 20 | 15 | 16 | 11 | 14 | 11 |
| Ni | 22 | 16 | 9 | 10 | 9 | 9 | 12 | 14 | 14 | 9 | 36 | 26 | b.d. | b.d. | 7 | b.d. | b.d. |
| Co | 1·7 | 1·8 | 2·0 | 2·3 | 1·3 | 1·4 | 2·0 | 3·9 | 4·5 | 3·4 | 54 | 26 | b.d. | 10 | 79 | 91 | 85 |

BVG: Bañobarez-Villavieja granites; Boh: Bohoyo granite; NavG: Navalonguilla granite.
PayG: El Payo granite; n.a.: not analysed; b.d.: below detection limit.

biotite, 991 °C ± 28 for internal cordierite-bearing, 1020 °C ± 42 for marginal cordierite-bearing and 1033 °C ± 66 for two-mica cordierite-bearing granites. This progressive increase in apparent apatite saturation temperature indicates that the most evolved compositions (marginal cordierite-bearing and two-mica cordierite-bearing granites) are furthest from apatite saturation, suggesting a progressively greater role for cumulate, xenocrystic or residual apatite phases during magmatic evolution.

## 4.2. Sr–Nd isotopes

Sr–Nd isotope data for the granites and nebulites are presented in Table 7. The isotope ratios were calculated at 306 Ma, the age of emplacement. Published representative Sr–Nd isotopic data of shales (Ugidos *et al.* 2003b) are also included in Table 7 for comparison.

The $(^{87}Sr/^{86}Sr)_{306}$ ratios for amphibole-bearing (0·7067–0·7070) and biotite granites (0·7062–0·7064) are comparable. Those of cordierite-bearing granites are variable and higher (0·7077–0·7089 and 0·7073–0·7094 for internal and marginal cordierite-bearing granites, respectively), except for one sample of the marginal cordierite-bearing biotite granite, which has a lower value (MC-10: 0·7066). The Bañobarez-Villavieja granites have a wide range (0·7049–0·7171). The $\varepsilon Nd_{306}$ values of amphibole-bearing (−4·4 to −3·6) and biotite granites (−4·2) are also comparable. There is more variation in the ratios of the cordierite-bearing granites that have higher values for the internal (−5·2 to −4·8) than for marginal (−6·3 to

https://doi.org/10.1017/S1755691009008159 Published online by Cambridge University Press

− 5·9), except for one sample of this group (MC-10: − 4·0) that has a value within the range of the amphibole-bearing granites. The $(^{143}Nd/^{144}Nd)_{306}$ ratios for the Bañobarez-Villavieja granites (− 3·8 to − 2·2) are similar to or higher than those of the amphibole-bearing and biotite granites. Most nebulite ratios (− 5·0 to − 3·8) are similar to those of the Upper Neoproterozoic shales (− 5·5 to − 4·4) while some (− 10·0 to − 6·5) are similar to those of the Lower Cambrian shales (− 9·4 to − 6·3).

The $(^{87}Sr/^{86}Sr)_{306}$–$\varepsilon Nd_{306}$ plot efficiently separates the Upper Neoproterozoic from the Lower Cambrian shales, nebulites, the Toledo pelites and the Layos granodiorite (Fig. 7). This again strongly suggests that the nebulites and the Layos granodiorite are compositionally equivalent to sedimentary rocks. The internal and marginal cordierite-bearing biotite granite plots deviate towards shales and the nebulites, whereas samples MC-10 (marginal cordierite-bearing granite) and VVA-11 (Bañobarez-Villavieja granites) plot close to the amphibole-bearing and biotite granites (Fig. 7). Relatively high $\varepsilon Nd_{306}$ values such as shown by sample MC-10 and the Bañobarez granites (Table 7) are not uncommon for other late Variscan peraluminous granites in the CIZ (Beetsma 1995; Donaire *et al.* 1999). However, other cordierite-bearing granites in the region show lower $\varepsilon Nd_{306}$ values (Beetsma 1995; Moreno-Ventas *et al.* 1995), as do the internal and marginal cordierite-bearing granites of this present work.

## 5. Discussion: the origin of cordierite-bearing granites in the CIZ

The convergence of isotopic and other compositional indicators in the cordierite granites towards those of the host metasedimentary rocks strongly suggests that the metasedimentary rocks are integrally involved in the petrogenesis of the cordierite granites, even if not at the present levels of exposure. In discussing the petrogenesis of the cordierite granites, it is convenient to address two end-member models, namely: (a) simple anatexis of country rocks; and (b) reactive assimilation of country rocks by another magma. Compositional variation attributable to fractional crystallisation is also considered.

### 5.1. Anatexis

The strongly peraluminous character of cordierite-bearing granites is frequently used to attribute such rocks to the melting of metasedimentary protoliths (Miller 1985). Field, mineralogical and geochemical evidence support the conclusion that the nubulites were derived from local metasedimentary rocks, but there are difficulties in reconciling the intrusive cordierite-bearing granites of this present study with simple anatexis of this source. Principal among these problems are stable isotope constraints on protoliths, major and trace element differences, and concerns over the source of heat required to melt metasedimentary protoliths of high chemical maturity.

Whole-rock $\delta^{18}O$ data for the principal rock types have previously been reported and the ranges are as follows: amphibole-bearing granites: +8·0 to +9·8‰; biotite granites: +7·7 to +9·5‰; internal cordierite-bearing biotite granites: +8·6 to +10·3‰; marginal cordierite-bearing biotite granites: +9·0 to +10·5‰; nebulites: +10·5 to +12·1‰; Upper Neoproterozoic shales: +11·6 to +13·8‰; Lower Cambrian shales: +9·3 to +12·4‰; and Lower Cambrian altered shales +10·0 to +14·3‰. These data indicate that very different protoliths are required to generate the cordierite-bearing granites compared with the nebulites (Recio *et al.* 1992). CaO is low and the Eu/Eu* ratio is high in the country rocks (shales, sandstones, nebulites), compared with cordierite-bearing granites, and these features would require selective enrichment of melts in CaO whilst retaining Eu in the residuum, a non-equilibrium process not known to occur on a regional scale. Upper Neoproterozoic and Lower Cambrian sedimentary rocks throughout Iberia are chemically highly mature (Valladares *et al.* 1993, 2002a, b; Beetsma 1995; Ugidos *et al.* 1997a, b; Bauluz *et al.* 2000) making them implausible protoliths for granites, with the possible exception of the leucogranites. Large-scale anatexis of such protoliths at shallow depths and subsequent mobilisation of magma requires considerable heat input and, in the absence of any evidence for significant volumes of contemporaneous basic rocks and seismic data, precludes the presence of significant quantities of mafic compositions in the crust of the CIZ (Banda *et al.* 1981, 1983). These objections make it difficult to reconcile the anatectic model with the available evidence.

Notwithstanding these problems with simple anatexis, if metasedimentary country rocks are the protoliths for these granites, an unusually large-scale homogeneous melting process must have selectively enriched the melt in Ca whilst retaining Eu in the restite. Furthermore, these cordierite-bearing granites have high FeO–MgO abundances and are much more mafic than minimum melts derived from upper crust metasedimentary protoliths through dehydration-melting reactions. If cordierite in the cordierite-bearing biotite granites is (at least in part) residual, then low P conditions (3–3·5 kbar) must be also accepted, given the absence of garnet in the granites and metasedimentary rocks as well as the relatively low Mg# of the country sedimentary rocks. The lack of significant volumes of contemporaneous basic magmas over the whole region makes it difficult to account for the necessary heat input at relatively shallow crustal levels by advection. If, on the other hand, garnet was left in the restite, there is a problem in explaining the absence of HREE fractionation in the cordierite-bearing biotite granites. Either way, cordierite-bearing biotite granites and biotite granites are chemically similar, for example the Zr contents and $(La/Yb)_n$ ratios in the biotite granites (cordierite absent) and the cordierite-bearing biotite granites largely overlap for most chemical parameters, and both are very different from their host rocks.

### 5.2. Assimilation

Field and petrographic similarities between cordierite in the nebulites and the cordierite granites (Fig. 4a, b), as well as field evidence for bulk assimilation (including gradual transitions between the biotite granites and cordierite-bearing biotite granites, transitional contacts between these late granites and nebulites, roof pendants of cordierite-rich migmatites in the cordierite-bearing biotite granites and the petrographic features of a cordieritite enclave isolated within an extensive biotite granite outcrop) all favour an origin of the cordierite granites by contamination of biotite granite magmas with cordierite-bearing country rocks, in particular the nebulites. It is proposed that the nebulites were melt-rich diatexites at the time of intrusion, facilitating the process of bulk assimilation of both melt and restitic component. Modelling the bulk compositions of all possible combinations of end members for a given fraction of contaminant using mass balance calculations allows the possibility of such extensive assimilation to be tested by comparing model compositions with the observed compositions of the cordierite granites.

The Sr–Nd isotope results are uniform for amphibole-bearing and biotite granites, but variable for cordierite-bearing granites that deviate towards sedimentary and nebulite the biotite granite compositions (Fig. 7), suggesting incorporation

https://doi.org/10.1017/S1755691009008159 Published online by Cambridge University Press

**Table 7** Sm–Nd and Rb–Sr isotope analyses of granites, nebulites and metasediments.

| Samples | Sm | Nd | $^{147}Sm/^{144}Nd$ | $^{143}Nd/^{144}Nd$ | ± 2 s | $^{143}Nd/^{144}Nd_{(306)}$ | $\varepsilon Nd_{(306)}$ | Rb | Sr | $^{87}Rb/^{86}Sr$ | $^{87}Sr/^{86}Sr$ | ± 2 s | $^{87}Sr/^{86}Sr_{(306)}$ | $^{87}Sr/^{86}Sr_{(543)}$ |
|---|---|---|---|---|---|---|---|---|---|---|---|---|---|---|
| NB | | | | | | | | | | | | | | |
| ABE-2 | 6·13 | 26·6 | 0·1392 | 0·512192 | 20 | 0·511913 | − 6·5 | 172 | 201 | 2·48 | 0·72310 | 4 | 0·712302 | 0·703907 |
| BOA-6 | 7·75 | 35·7 | 0·1314 | 0·511989 | 7 | 0·511726 | − 10·1 | 174 | 203 | 2·49 | 0·72818 | 4 | 0·717359 | 0·708946 |
| I-30 | 7·21 | 33·9 | 0·1288 | 0·512255 | 6 | 0·511997 | − 4·8 | 125 | 132 | 2·75 | 0·72943 | 4 | 0·717473 | 0·708177 |
| AG | | | | | | | | | | | | | | |
| MIRA-3 | 7·86 | 37·8 | 0·1259 | 0·512309 | 23 | 0·512057 | − 3·7 | 145 | 204 | 2·06 | 0·71596 | 5 | 0·706998 | |
| CARA-1 | 6·02 | 25·7 | 0·1417 | 0·512301 | 21 | 0·512017 | − 4·5 | 164 | 158 | 3·01 | 0·71980 | 4 | 0·706707 | |
| CARA-6 | 5·62 | 23·8 | 0·1429 | 0·512301 | 20 | 0·512015 | − 4·5 | 165 | 144 | 3·32 | 0·72149 | 3 | 0·707034 | |
| BG | | | | | | | | | | | | | | |
| VAA-5 | 7·41 | 38·2 | 0·1174 | 0·512267 | 6 | 0·512032 | − 4·1 | 175 | 190 | 2·67 | 0·71803 | 2 | 0·706414 | |
| MIRA-5 | 7·75 | 35·5 | 0·1319 | 0·512299 | 20 | 0·512035 | − 4·1 | 168 | 167 | 2·91 | 0·71891 | 1 | 0·706221 | |
| ICG | | | | | | | | | | | | | | |
| BEU-17 | 6·83 | 32·2 | 0·1282 | 0·512233 | 6 | 0·511976 | − 5·2 | 166 | 178 | 2·70 | 0·72074 | 4 | 0·708975 | |
| BEU-16 | 6·66 | 29·8 | 0·1353 | 0·512273 | 6 | 0·512002 | − 4·7 | 200 | 131 | 4·43 | 0·72702 | 4 | 0·707748 | |
| PHU-1 | 5·11 | 21·5 | 0·1438 | 0·512285 | 7 | 0·511997 | − 4·8 | 212 | 106 | 5·80 | 0·73414 | 4 | 0·708876 | |
| MCG | | | | | | | | | | | | | | |
| XSA-9 | 6·01 | 27·8 | 0·1306 | 0·512205 | 20 | 0·511943 | − 5·9 | 277 | 151 | 5·32 | 0·73262 | 4 | 0·709451 | |
| MC-13 | 5·29 | 24·1 | 0·1328 | 0·512185 | 8 | 0·511919 | − 6·4 | 275 | 171 | 4·66 | 0·72767 | 4 | 0·707369 | |
| MC-10 | 7·89 | 35·5 | 0·1346 | 0·512310 | 24 | 0·512040 | − 4·0 | 233 | 154 | 4·39 | 0·72573 | 4 | 0·706634 | |
| BVG | | | | | | | | | | | | | | |
| VVA-11 | 4·47 | 18·9 | 0·1433 | 0·512343 | 6 | 0·512056 | − 3·7 | 313 | 40 | 22·69 | 0·803753 | 19 | 0·704946 | |
| CBH-10 | 3·88 | 15·9 | 0·1477 | 0·512345 | 6 | 0·512049 | − 3·8 | 298 | 45 | 19·20 | 0·800776 | 34 | 0·717167 | |
| CBH-38 | 6·24 | 28·1 | 0·1344 | 0·512402 | 10 | 0·512133 | − 2·2 | 249 | 80 | 9·03 | 0·750382 | 20 | 0·711059 | |
| LC | | | | | | | | | | | | | | |
| GU-22 | 8·07 | 46·4 | 0·1053 | 0·511971 | 6 | 0·511760 | − 9·4 | | | | | | | |
| GU-23 | 7·11 | 38·2 | 0·1127 | 0·512005 | 7 | 0·511779 | − 9·1 | | | | | | | |
| GU-26 | 7·72 | 39·3 | 0·1189 | 0·511997 | 7 | 0·511759 | − 9·5 | | | | | | | |
| SSA-2 | 16·44 | 78·6 | 0·1266 | 0·512261 | 6 | 0·512007 | − 4·6 | | | | | | | |
| SSA-13 | 18·06 | 78·3 | 0·1396 | 0·512224 | 7 | 0·511944 | − 5·8 | | | | | | | |
| SSA-15 | 10·01 | 48·7 | 0·1243 | 0·512164 | 6 | 0·511915 | − 6·4 | | | | | | | |
| SSA-20 | 6·83 | 33·1 | 0·1250 | 0·512075 | 6 | 0·511825 | − 8·2 | | | | | | | |
| SSA-30 | 7·80 | 38·4 | 0·1230 | 0·512138 | 6 | 0·511892 | − 6·9 | | | | | | | |
| SSA-24 | 8·32 | 43·0 | 0·1170 | 0·512095 | 6 | 0·511861 | − 7·5 | | | | | | | |
| SIA-11 | 8·78 | 40·8 | 0·1301 | 0·512136 | 6 | 0·511875 | − 7·2 | | | | | | | |
| CR-5 | 6·76 | 34·9 | 0·1172 | 0·512092 | 6 | 0·511857 | − 7·5 | | | | | | | |
| UN | | | | | | | | | | | | | | |
| HR-41 | 7·49 | 36·0 | 0·1260 | 0·512270 | 8 | 0·512018 | − 4·4 | | | | | | | |
| HR-45 | 6·19 | 28·4 | 0·1321 | 0·512229 | 6 | 0·511964 | − 5·5 | | | | | | | |
| SSA-12 | 11·99 | 56·3 | 0·1287 | 0·512221 | 9 | 0·511963 | − 5·5 | | | | | | | |
| SIA-31 | 7·35 | 39·5 | 0·1127 | 0·512186 | 6 | 0·511960 | − 5·5 | | | | | | | |
| SIA-22 | 7·56 | 36·6 | 0·1250 | 0·512270 | 7 | 0·512020 | − 4·4 | | | | | | | |
| SIA-25 | 7·96 | 36·8 | 0·1310 | 0·512220 | 7 | 0·511958 | − 5·6 | | | | | | | |
| SIA-3 | 8·14 | 40·7 | 0·1209 | 0·512191 | 9 | 0·511949 | − 5·8 | | | | | | | |
| SIA-33 | 12·38 | 50·9 | 0·1472 | 0·512244 | 9 | 0·511949 | − 5·8 | | | | | | | |
| FG-4 | 8·96 | 42·5 | 0·1274 | 0·512272 | 7 | 0·512017 | − 4·4 | | | | | | | |

NB: Nebulites; AG: Amphibole-bearing biotite granites; BG: Biotite granites; ICG: Internal cordierite-bearing biotite granites; MCG: Marginal cordierite-bearing biotite granites; BVG: Bañobarez-Villavieja cordierite-bearing two mica granites; LC: Lower Cambrian shales; UN: Upper Neoproterozoic shales (corrected data from Table 3 in Ugidos *et al.* 2003b).

of these materials into the biotite granite. The isotopic heterogeneity of the resulting granites following assimilation is attributable to the wide compositional variation shown by the likely contaminants of the granites (Upper Precambrian and/or Lower Cambrian shales, reworked phosphate-rich rocks, altered shales). These end-members are sufficient to explain the observed compositional variation in the unevolved internal cordierite-bearing granites. Application of mixing models to $\varepsilon Nd_{306}$ and $^{87}Sr/^{86}Sr_{306}$ indicate that the bulk assimilation of 10–25% nebulite can account for the compositions of the internal cordierite-bearing granites (Fig. 7). However, such assimilation modelling using the range of biotite granites and nebulite compositions does not account for all the marginal cordierite-bearing granite samples; some of these differences are discussed below in terms of unusual contaminant compositions. All available isotopic data, including stable isotopes (see Recio *et al.* 1992), are consistent with the cordierite-bearing granites, being mixtures of biotite granites and host rocks.

The assimilation model is further tested using the available major and trace elements, a selection of which (including trace element ratios) is presented in Figures 8 and 9. The shaded areas encompass compositions generated by the assimilation of 10% nebulite into the range of biotite granites. These diagrams show that almost all the internal cordierite-bearing granite samples are adequately modelled and most samples that do not fall within this model field lie very close, although there are a few outliers, as might be expected in such a heterogeneous system. As with the isotopic modelling, no combination of nebulite assimilant and biotite granite host magma is capable of replicating the major and trace element compositions of all the marginal cordierite-bearing granites.

In several variation diagrams the biotite granites suggest a fractionation trend, and all granite types and the nebulites overlap this same trend. Examples are the $SiO_2$–$TiO_2$, $SiO_2$–Zr and Zr–LREE diagrams (Fig. 8a, c, b). However, in other diagrams, such as $SiO_2$–Y, Zr–HREE and Zr–Sm/Nd (Fig. 8e, d, f), while the data mostly overlap the biotite granites and internal cordierite-bearing granites, plots are rather scattered and describe only broad general trends. $SiO_2$–Y and Zr–HREE plots indicate two groups of samples, each including marginal cordierite-bearing and Bañobabarez and Villavieja granites, that are characterised by relatively high and low Y and HREE contents. These results are difficult to reconcile with a simple fractionation model since, in principle, Zr–HREE rather than Zr–LREE correlation is expected for zircon fraction, for example. Thus, it is suggested that the abundances of zircon and LREE-carriers are both dependent on the contents of inherited accessories (probably as inclusions) entrained in the rising magma, and also on the closure effect, rather than on magmatic precipitation. The tight trend defined in Figure 8b suggests a close relationship between all granites. It is important to highlight that samples rich in Y and HREE correspond to the marginal cordierite-bearing and the two-mica cordierite-bearing bodies that intrude Lower Cambrian units that are chemically anomalous, in particular in their relatively high abundances of Y and HREE (see section 1).

In diagrams where the nebulites and biotite granites trends diverge (Fig. 9), the marginal cordierite-bearing granites tend to plot with intermediate values (e.g., CaO–$SiO_2$, CaO–$Fe_2O_3$, CaO–Zr, CaO–Rb/Sr, CaO–Eu/Eu*, CaO–Sm/Nd). Most diagrams indicate that magmatic fractionation links the internal, marginal, and two-mica cordierite-bearing granites, and intense fractionation is suggested for the most evolved rocks by the CaO–Rb/Sr diagram (Fig. 9d). Variation diagrams, including $P_2O_5$, suggest more complex relationships. $SiO_2$–$P_2O_5$ and CaO–$P_2O_5$ exhibit negative correlations for biotite granites,

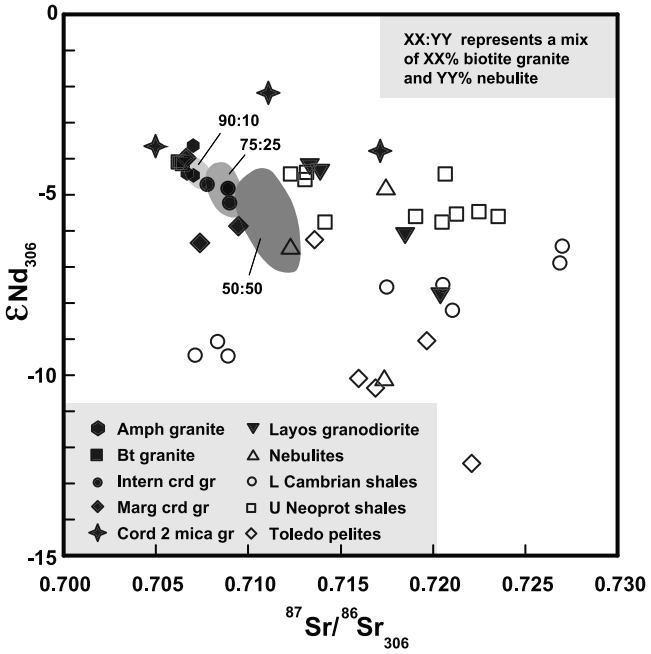


**Figure 7** Sr–Nd isotope ratios for the granites and host rocks including Upper Neoproterozoic shales, Lower Cambrian shales, Toledo pelites and nebulites. Granites include amphibole-bearing biotite granite (Amph granite), biotite granite (Bt granite), internal cordierite-bearing biotite granite (Intern crd gr), marginal cordierite-bearing biotite granite (Marg crd gr), cordierite-bearing two-mica granites (Cord 2 mica gr) and the Layos granodiorite. Isotopic data for the Layos granodiorite and the Toledo pelites taken from Barbero *et al.* (1995) and Villaseca *et al.* (1998). Rb–Sr data for the Upper Neoproterozoic and Lower Cambrian shales taken from Ugidos *et al.* (2003b). The shaded fields encompass all compositions generated by mixing Bt granite samples with 10%, 25% and 50% nebulites respectively for all combinations of Bt granite and nebulite samples.

while marginal and cordierite-bearing two-mica granites have higher $P_2O_5$ concentrations than biotite granites for the same $SiO_2$ or CaO (Fig. 10). The $Al_2O_3$–$P_2O_5$ diagram (Fig. 10b) shows negative covariation for the biotite granite, but $Al_2O_3$ remains essentially constant in the marginal and two-mica cordierite-bearing granites with varying $P_2O_5$. None of the trace elements show significant covariation with $P_2O_5$ in these granites. The REE patterns (Fig. 11) in the nebulites, biotie granites and most internal cordierite-bearing granites are broadly similar, whereas some of the marginal and the cordierite-bearing two-mica granites have more complex HREE patterns consistent with results above.

In any assimilation model, a major constraint is the volume of contaminant required to explain the petrological and geochemical features of the product. Large degrees of contamination are not required to account for the field observations on the spatial density of cordierite that ranges from 20 to 74 prisms/$m^2$ in the marginal cordierite-bearing granites. Given that the average size of cordierite prism in these granites is about 1·5 $cm^2$, the cordierite content of this granite is about 1·1 vol. % on a regional scale, requiring 11 vol. % assimilation of a contaminant with 10% modal cordierite; the range of cordierite abundance in nebulites is 10–20%. If cordieritites (60–80% modal cordierite) were the only contaminant, assimilation of less than 1·8 vol. % of these rocks would be sufficient to introduce up to 1·1 vol. % of cordierite. The effects on trace element contents would be undetectable, especially in those examples where data on granite and contaminant overlap. The data indicate strong controls exerted by contaminant composition and the inheritance of accessory minerals, but the most evolved facies may also require a stage of crystal-liquid fractionation.

https://doi.org/10.1017/S1755691009008159 Published online by Cambridge University Press

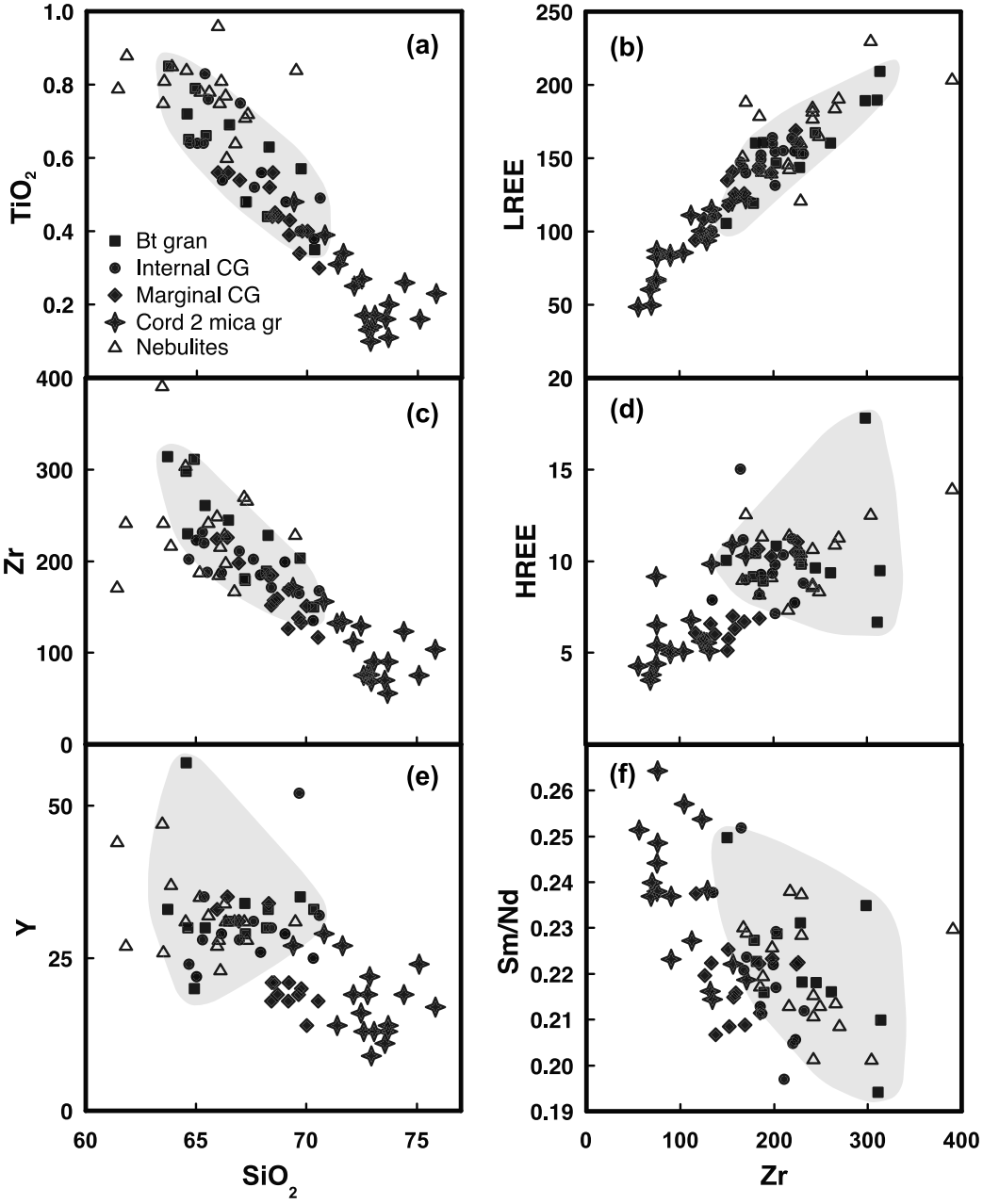


**Figure 8** Variation diagrams for granites and nebulites. Bt gran: Biotite granites; Internal CG: Internal cordierite-bearing biotite granites; Marginal CG: Marginal cordierite-bearing biotite granites; Cord 2 mica gr: small cordierite-bearing two-mica granites, including the Bañobarez-Villavieja, Bohoyo, Navalonguilla and El Payo granites. The shaded field encompasses all compositions generated by mixing Bt granite samples with 10% nebulites for all combinations of Bt granite and nebulite samples.

### 5.3. Fractional crystallisation

The assimilation model for the cordierite granites does not fully account for the marginal cordierite granites, or the two-mica cordierite-bearing granites. The marginal cordierite-bearing granites evolve to higher silica and lower $TiO_2$, Zr, Y, LREE and HREE than the nebulite and biotite granite end-members, whereas the two mica cordierite-bearing granites are generally significantly more evolved than the marginal cordierite granites and very depleted in Zr and the rare earths (Figs 8, 9). Such evolved compositions cannot be achieved solely by assimilation and it is necessary to invoke an igneous differentiation process, although there is convincing field and geochemical evidence for the late involvement of assimilation in the marginal cordierite-bearing granites. Zr, Hf, Th, LREE and HREE depletion with increasing $SiO_2$ implicates zircon and monazite removal; whereas the exponential increase in Rb/Sr, as well as rapid declines in $TiO_2$, $Fe_2O_3$, and CaO (Figs 8, 9), attests to mafic mineral and feldspar removal. Severe depletion in the HREE may also indicate the removal of garnet. The removal of these minerals differentially to create the observed trends in the biotite granites may have occurred for residual phases at or close to the source, or by crystal fractionation at a higher level. Residual mineral control is favoured if HREE depletion was due to the retention of garnet in the source. Alternatively, linear trends in Y and HREE within the marginal cordierite-bearing granites could be explained by variable assimilation of local metasedimentary rocks that range from Y- and HREE-depleted to horizons that are anomalously enriched in these elements. Quantitative models of combined assimilation and fractional crystallisation (DePaolo 1981) was not attempted because the heterogeneity of both assimilant and host rock mean that individual samples cannot represent the range of compositions involved. Furthermore, such models depend on accurate knowledge of crystal-

https://doi.org/10.1017/S1755691009008159 Published online by Cambridge University Press

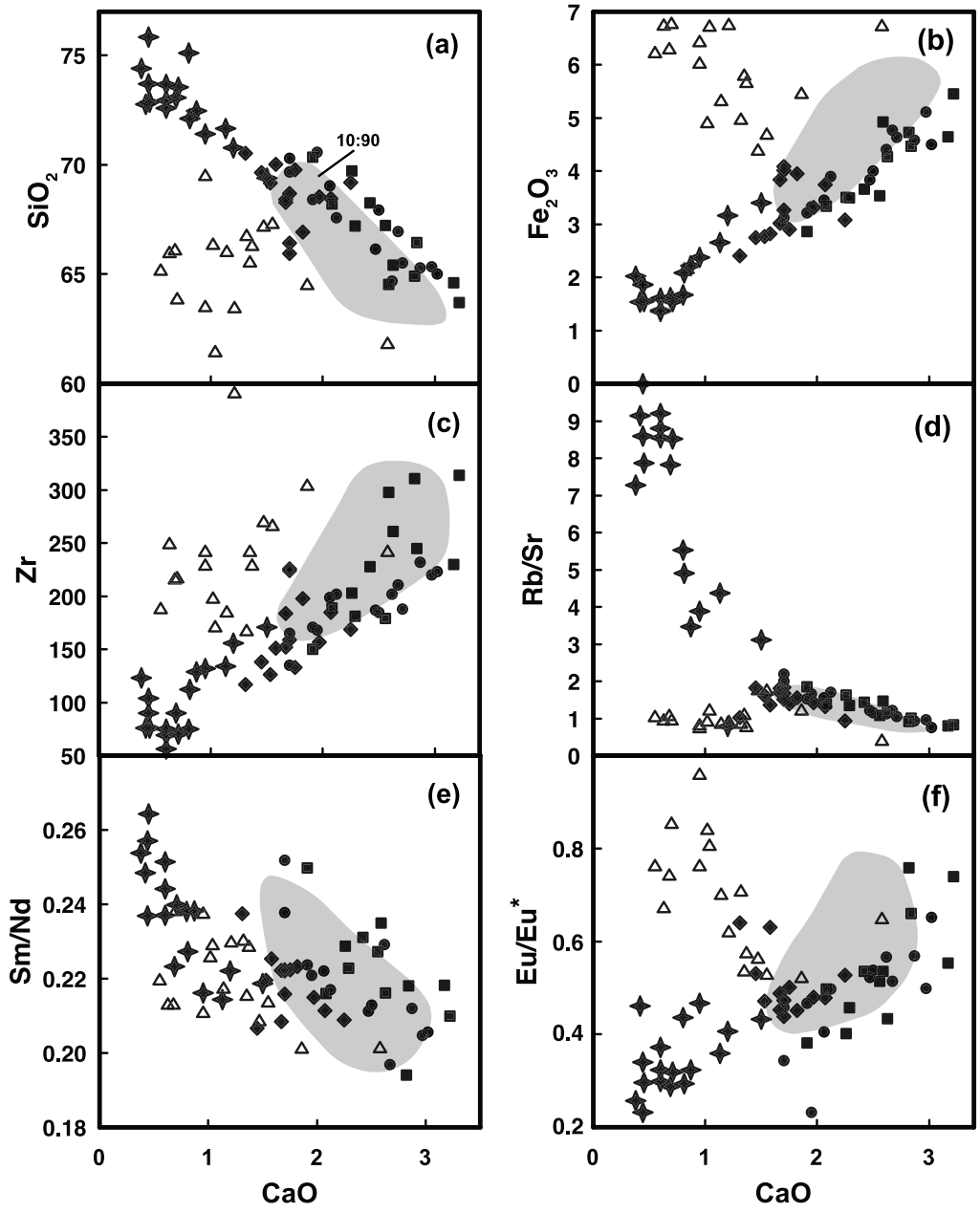


**Figure 9** Comparison of variation trends in granites with those in nebulites. Symbols and shading as for Figure 8.

liquid partitioning and this is not available for several important trace elements. A significant fraction of zircon, the main repository of Zr, is inherited, and the rare earths and Th are major components of monazite and do not conform to Henry's Law. Trace element abundances and radiogenic isotope trends are however qualitatively consistent with a model in which the marginal cordierite-bearing granites are derived from these differentiated biotite granites through the assimilation of the nebulites and other metasedimentary rocks in broadly similar quantities as required to generate the internal cordierite-bearing granites (up to 20%).

### 5.4. Influence of host rock compositions

Phosphate deposition is recorded on nearly all continents during the Late Proterozoic and Lower Cambrian, frequently associated with changes in sea level (Cook & Shergold 1986; Cook 1992). High phosphate concentrations (13 to 24% $P_2O_5$) are also found in western Spain (Perconig *et al.* 1986; Gabaldón *et al.* 1989) as well as in the present study area (Oczlon & Díez Balda 1992; Rodríguez Alonso *et al.* 2004). Primary phosphorites have low REE abundances, whereas post-depositional weathering, reworking, interaction with ground waters, and diagenesis can lead to significant REE (including Y) removal and redistribution (McArthur 1980; Ilyin 1998; Rasmussen *et al.* 1998) with consequent modification of trace element ratios, including Sm–Nd fractionation and neodymium isotope resetting on a regional scale (Bouch *et al.* 1995; Bock *et al.* 1998; Lev *et al.* 1999). Table 3 includes samples with variable trace element abundances, especially the REE (and their ratios), comparable to the altered detrital samples in Table 2. It is suggested that REE redistribution during diagenesis is the likely cause of this variability. Possible examples of neodymium isotope resetting in host rocks are the samples SSA-2 and SSA-13 that have anomalous REE (including Y) abundances (Table 2) and the highest $(^{143}Nd/^{144}Nd)_{306}$ ratios (Table 7) among the Lower Cambrian shales. The influence of rare earth composition is illustrated by samples MC-10 and CBH-38 (marginal and two-mica cordierite-bearing granites, respectively) that have the highest $(^{143}Nd/^{144}Nd)_{306}$ ratios of their respective granite groups (Table 7) as well as the highest Y contents (Tables 5 and 6).

https://doi.org/10.1017/S1755691009008159 Published online by Cambridge University Press

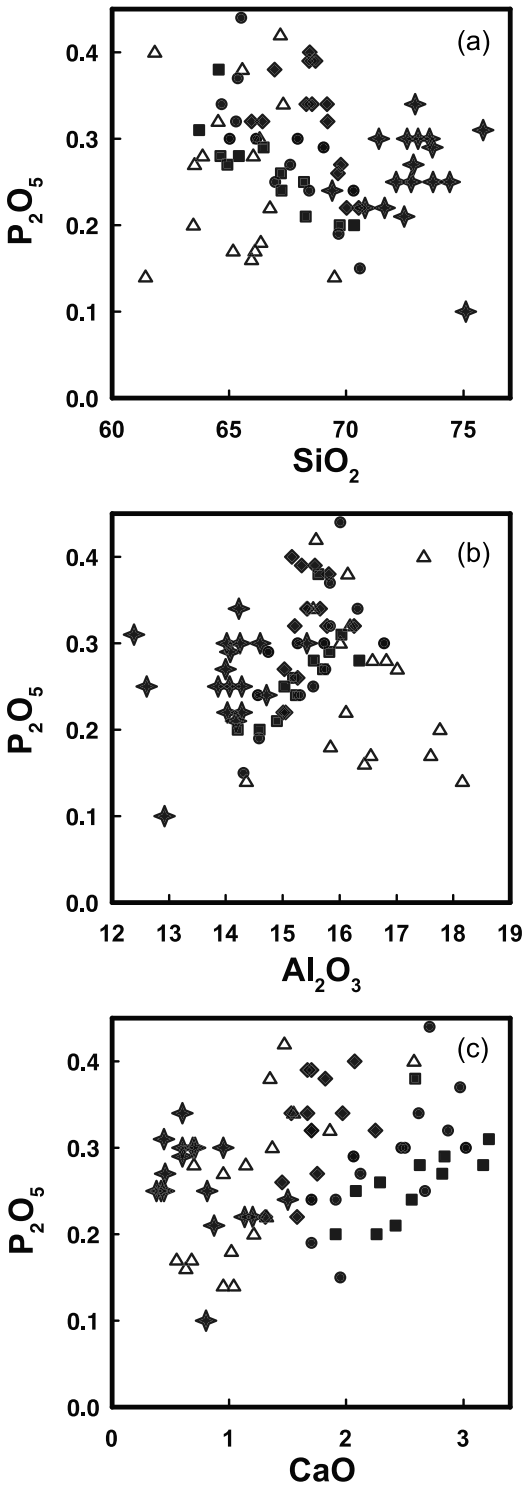


**Figure 10** Variation of $P_2O_5$ with some other major oxides. Symbols as for Figure 8.

The relatively high $P_2O_5$ content of the cordieritites is consistent with an origin by contamination involving P-rich sedimentary layers. The relatively high REE contents (Table 4) and the lack of negative cerium anomalies in the cordieritites contrast with the chemical features of primary marine phosphates, but are also features of the phosphate-rich rocks in Table 4. Thus the geochemical features shared by the altered detrital and phosphate-rich rocks and cordieritites suggest that protoliths of the latter mainly consisted of reworked and altered sediments, and the data are consistent with an origin of the cordieritites in low-P–high-T metamorphism of specific, chemically mature sedimentary beds.

The trends defined by the internal and marginal cordierite-bearing, and the Bañobarez-Villavieja granites in the $SiO_2$–$P_2O_5$, $P_2O_5$–$Al_2O_3$ and CaO–$P_2O_5$ plots (Fig. 10) are not consistent with simple magmatic fractionation trends, whereas such trends are apparent in the biotite granites. The relatively high $P_2O_5$ contents in many samples of the cordierite-bearing and cordierite-bearing two-mica granites probably resulted from a combination of processes, including assimilation of the P-rich country rocks and the behaviour of P in the new melt after Al dissolution. The assimilation of aluminophosphates reported in Central Portugal (Gama Pereira 1984) and the presence of P-rich rocks as enclaves in the biotite granites, also supports such a process. The range of P concentrations in the host material may be wide, as may be the ranges of many other elements (REE, Y, Th, U, etc), depending on whether phosphate minerals are primary or secondary and on the redistribution of trace elements in the assimilated rocks. The Y contents in altered Lower Cambrian shales are three- to six-fold higher than those of unaltered shales. Thus, the two trends are apparent in the $SiO_2$–Y diagram (Fig. 8e) but the marginal cordierite-bearing and two-mica cordierite-bearing granites may relate to contaminants with different Y abundances and subsequent fractionation. An important aspect is that the incorporation of small quantities of cordierite-bearing rocks would dramatically modify the range of $P_2O_5$ abundance in granites, and would introduce new minerals such as cordierite and andalusite.

The question of the extent of highly reworked and altered sediments in the host sequence is relevant to the probability of assimilating unusual compositions. Those corresponding to the Neoproterozoic–Cambrian transition are well characterised, but the results of sequence stratigraphy studies (see section 1) suggest that the lower sequence boundary of the Neoproterozoic sequence would also be an unconformity related to a fall in sea level, and the sediments may have similarly acquired extreme compositional characteristics. The relationships between stratigraphic units and the stratigraphic levels into which the granites of the Central Iberian Zone in the region W and S of Salamanca were emplaced are summarised in Table 1. This stratigraphic framework could explain the presence elsewhere of some cordierite-bearing granites within Precambrian series rocks that have clearly not traversed the extreme compositions observed at the Neoproterozoic–Cambrian boundary. Given that the peak of metamorphism postdates the folding phases, then P–T conditions at both sequence boundaries may have been similar. Thus, granite magmas emplaced in both lower and upper sequence boundaries may have experienced similar compositional and thermal environments.

### 5.5. Origin of the cordierite-rich rocks

Many examples of cordierite-rich host rocks have been reported in the literature. Examples include: partially melted cordierite-rich pelitic hornfelses and restites having up to 40% (euhedral) and 60–90% cordierite, respectively (Riesco *et al.* 2004); cordierite crystals and partially melted xenoliths with 12–34% cordierite (Gribble 1968); gneisses with up to 32% cordierite (Fediuk 1971; Blümel & Schreyer 1977); leucosomes in thermal aureoles with abundant euhedral cordierite porphyroblasts up to 1 cm long (Evans & Speer 1984); basic granulites with 20–28% cordierite (Davidson & Mathison 1974); migmatites with up to 41% cordierite (Jamieson 1984); and cordieritites with 60–90% cordierite (Gordillo 1979; Schreyer *et al.* 1979; Ugidos 1988; Rapela *et al.* 2002; Droop *et al.* 2003). Rocks of extreme composition, such as emery-like rocks with $Al_2O_3$ 32–53%, $Fe_2O_3$ (total) 15–27%, MgO 2·4–8·5% (Smith 1965) and high-grade average metamorphic rocks with $Al_2O_3$

https://doi.org/10.1017/S1755691009008159 Published online by Cambridge University Press

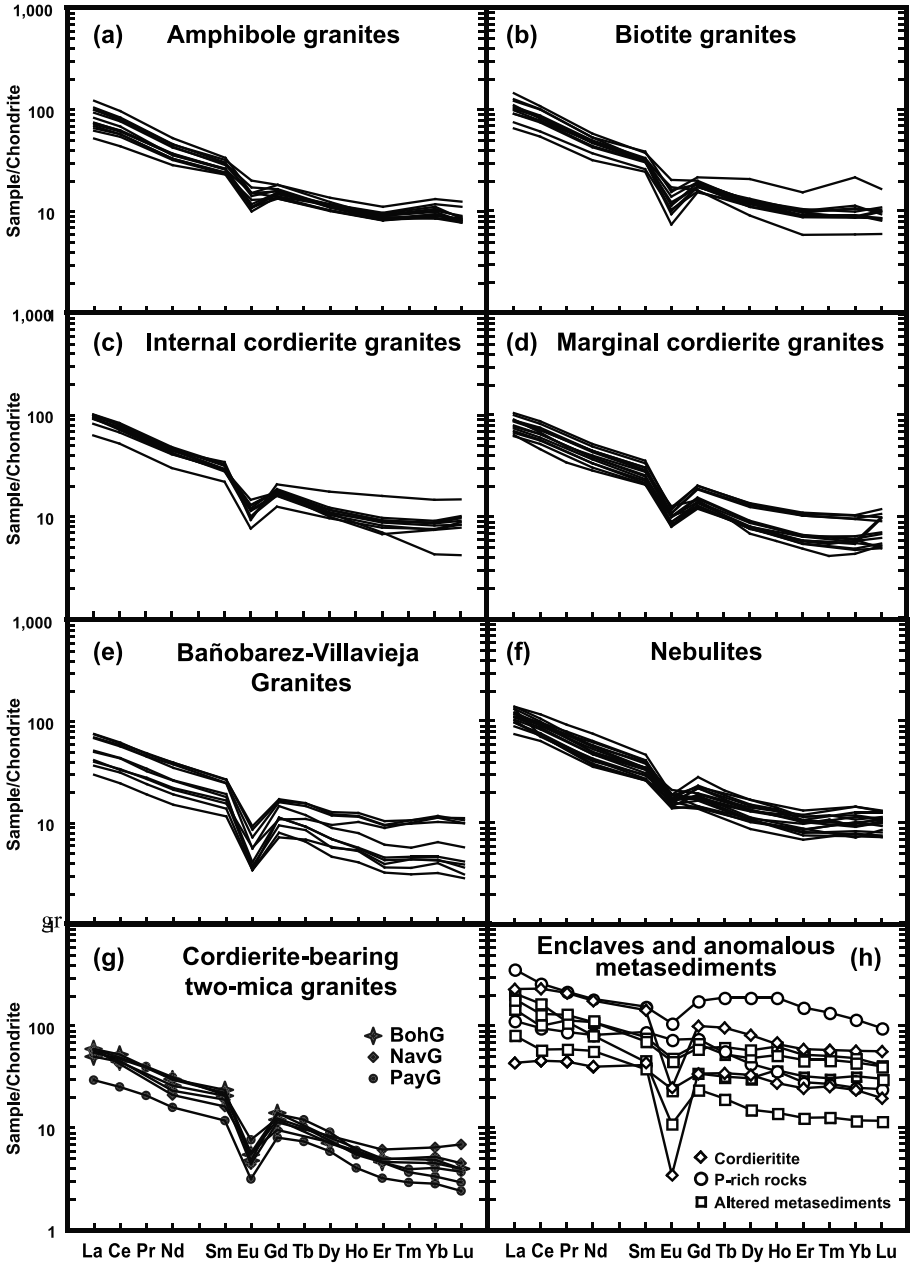


**Figure 11** Chondrite-normalised REE patterns for the major rock types: (a) amphibole granites; (b) biotite granites; (c) internal cordierite-bearing granites; (d) marginal cordierite-bearing granites; (e) Bañobarez-Villavieja two-mica cordierite-bearing granites; (f) nebulites, (g) El Payo granite (PayG), Navalonguilla granite (NavG) and Bohoyo granite (BohG); (h) cordieritite enclaves and some anomalous Lower Cambrian rocks. Normalisation values for chondrite from Taylor & McLennan (1985).

44%, FeO* 11·0%, MgO 5·8% have been reported (Nell 1985). In most of these examples, the origin of the extreme bulk composition has been attributed to the loss of a leucogranitic melt fraction, and cordierite is considered to be a solid product of incongruent biotite-consuming reactions. However, this interpretation is based mainly on major element data, and there are few studies indicating a restitic origin on the basis of element ratios in low-grade (or unmetamorphosed) and equivalent high-grade (or inferred restitic) rocks.

The melt loss model is testable in that restites would be expected to become relatively enriched in refractory elements, as compared with their protoliths, following the generation and migration of a leucogranitic melt. In fact, the cordieritites of this study have similar Mg#, lower $TiO_2$, V, Cr, Ni and Cu abundances and lower Eu/Eu* ratios than the shales and nebulites. Thus the cordieritites cannot be restitic rocks resulting from melt extraction after melting of the shales, sandstones and nebulites. A model more consistent with the data is that these cordieritites are original reworked and altered detrital rocks, as are SSA-7 and SSA-8 above. It is suggested here that intense alteration of sediments with subsequent accumulation of clay-rich horizons would result in bulk compositions similar to those interpreted above as 'melt depleted' restites, and such protolith compositions may actually account for many cordierite-rich occurrences. Other cordieritite types may develop from biotite+sillimanite-rich restitic rocks; indeed, cordierite-rich rocks are common and are not necessarily restitic, but may be high-grade hornfelses or migmatites from undepleted country rocks. Contaminants in the formation of cordierite granites in this present study include high-grade hornfelses, nebulites, cordieritites from altered sedimentary beds, as well as restitic cordieritites.

https://doi.org/10.1017/S1755691009008159 Published online by Cambridge University Press

### 5.6. Thermal considerations

Large-scale assimilation of host rocks by intruding granites magmas is usually considered implausible, given the relatively low temperatures of granite magmas and the high melting temperatures of siliceous country rocks. More widely accepted is the assimilation of host rocks by basic magmas through the partial melting of xenoliths. Thermal contrasts between country rocks and magma cause stresses which assist the fracturing of the country rocks (Furlong & Myers 1985), and dehydration melting reactions in xenoliths facilitate their assimilation through the disintegration of xenoliths and the dispersion of the melt and xenocrysts in the host magma (Green 1994). Extensive reaction of xenocrysts with the host melt phase generates a new mineral assemblage that will be difficult to detect as initially derived from the contaminant. This reactive bulk assimilation model (Beard *et al*. 2005) has a much smaller thermal requirement than conventional assimilation models (Grove *et al*. 1988), but may be very difficult to detect because extensive re-equilibration of the solid phases with the host melt tends to obliterate original features that may be linked to the contaminant. The features most likely to persist are the radiogenic isotope ratios and some trace elements, although significant increase in modal cordierite towards the outer contacts with pelitic host rocks, as described in section 3.4, strongly supports the assimilation model.

A recent analysis of the thermal limitations on wall rock assimilation by basaltic magma (Glazner 2007) found that the process would most likely be limited by the effect of crystal content on viscosity, and thus restricted to a few tens of percent incorporation of xenoliths. It is quite common, as in the region studied, for peak metamorphic conditions to postdate the compressive phases of orogenies, and for the maximum volume of granite magma to be emplaced contemporaneously with the extensional stages. This implies that the pressure decrease coincided with the ascent of late orogenic voluminous granite magmas from deep crustal sources that were probably emplaced at similar depths in the middle/upper crust. Thus, the evolution of regional metamorphism from intermediate to low P is coincident with thermal advection by granite magmas. As a consequence, relatively high regional isotherms/isograds may have been telescoped, while the decrease in pressure would have facilitated biotite–muscovite- and biotite–sillimanite-consuming reactions, resulting in high-T–low-P cordierite-rich ($\pm$ andalusite) rocks such as high-grade hornfelses, cordieritites, migmatitic hornfelses and, for the nebulites, fluid-absent melting reactions (positive slopes). The same reactions affecting the sillimanite + biotite restitic associations from earlier leucogranites may have generated restitic cordieritites.

Phyllosilicate-consuming reactions under subsolidus conditions produce alkali feldspar and $H_2O$ that in turn may lower solidus temperatures and facilitate the generation of some inter-crystalline melt in the host rocks and within xenoliths (Buick *et al*. 2004). Enclaves of host rocks up to 10 m long are present in the cordierite granites of the study area, and these were subject to Variscan metamorphism prior to incorporation as stoped blocks in the granite magma. This situation is optimal for achieving extensive reactive assimilation. Less than optimal would be the generation of largely structureless high-grade rocks in thermal aureoles without an interstitial melt phase. Under these circumstances, the stresses caused by thermal and dilation anisotropy of minerals on magma emplacement (Ugidos 1988; Clarke *et al*. 1998), together with the mechanical effects of shear stress and thermo-chemical abrasion during the sinking of host rock blocks in the magma, will facilitate the disaggregation of cordierite-rich rocks into dispersed xenocrysts.

## 6. Concluding remarks

In conclusion, the occurrence of regional-scale cordierite granites is explained with a model involving extensive reactive assimilation of nebulites by biotite granite magma. The process of reactive assimilation reduces the thermal requirements as compared with bulk assimilation, and may be applicable to granites when the thermal requirements are lowered still further for magmas that are emplaced into high temperature rocks close to solidus conditions. A consequence of the reactive assimilation process is that much of the evidence is destroyed, however isotopic contrasts and other chemical features are preserved in the cordierite granites of the Central Iberian Zone that are wholly consistent with this process.

## 7. Acknowledgements

Felix García and Donald Herd are thanked for assistance with the microprobe analyses. Financial support for this work was provided by the EU Science Programme (Project SCI-CT90-0397) and PB 91-0321 project of the MEC (Spain). The manuscript has benefited from suggestions by Antonio Castro and an anonymous referee.

## 8. References

Banda, E., Suriñac, E., Aparicio, A., Sierra, J. & Ruiz de la Parte, E. 1981. Crust and upper mantle structure of the Central Iberian Meseta (Spain). *Geophysical Journal of the Royal Astronomical Society* **67**, 779–89.

Banda, E., Udías, A., Mueller, S., Mezcua, J., Boloix, M., Gallaert, J. & Aparicio, A. 1983. Crustal structure beneath Spain from deep seismic sounding experiments. *Physics of the Earth and Planetary Interiors* **31**, 277–80.

Barbero, L., Villaseca, C., Rogers, G. & Brown, P. E. 1995. Geochemical and isotopic disequilibrium in crustal melting: An insight from the anatectic granitoids from Toledo, Spain. *Journal of Geophysical Research* **100**, 15,745–65.

Barbero, L. & Villaseca, C. 1992. The Layos granite, Hercynian complex of Toledo (Spain): an example of parautochtonous restite-rich granite in a granulitic area. *Transactions of the Royal Society of Edinburgh: Earth Sciences* **83**, 127–38.

Bauluz, B., Mayayo, M. J., Fernández-Nieto, C. & González López, J. M. 2000. Geochemistry of Precambrian and Paleozoic siliciclastic rocks from the Iberian Range (NE Spain): implications for source-area weathering, sorting, provenance and tectonic setting. *Chemical Geology* **168**, 135–50.

Beard, J. S., Ragland, P. C. & Crawford, M. L. 2005. Reactive bulk assimilation: A model for crust-mantle mixing in silicic magmas. *Geology* **33**, 681–4.

Beetsma, J. J. 1995. *The Late Proterozoic/Paleozoic and Hercynian crustal evolution of the Iberian Massif, N Portugal*. PhD Thesis, Vrije University, Amsterdam.

Blümel, P. & Schreyer, W. 1977. Phase relations in pelitic and psammitic gneisses of the sillimanite–potash feldspar and cordierite-potash feldspar zones in the Moldanubicum of the Lam–Bodenmais area, Bavaria. *Journal of Petrology* **18**, 431–59.

Bock, B., McLennan, S. M. & Hanson, G. N. 1998. Geochemistry and provenance of the Middle Ordovician Austin Glen Member (Normanskill Formation) and the Taconic Orogeny in New England. *Sedimentology* **45**, 635–55.

Bouch, J. E., Hole, M. J. & Trewin, N. A. C. 1995. Low temperature aqueous mobility of the rare-earth elements during sandstone diagenesis. *Journal of the Geological Society, London* **152**, 895–8.

Bowen, N. L. 1928. *The evolution of the igneous rocks*. New York: Dover Publications.

Buick, I. S., Stevens, G. & Gibson, R. L. 2004. The role of water retention in the anatexis of metapelites in the Bushveld Complex Aureole, South Africa: an experimental study. *Journal of Petrology* **45**, 1777–97.

Carnicero, A. 1982. Estudio del metamorfismo existente en torno al granito de Lumbrales. *Stvdia Geologica Salmanticensia* **17**, 7–20.

Carnicero, A. 1983. *Síntesis geológica del basamento E: 1/200000* (*Zona del Centro-Oeste español*). Universidad de Salamanca: Departamento de Petrología.

https://doi.org/10.1017/S1755691009008159 Published online by Cambridge University Press

Carnicero, A., López-Plaza, M. & Delgado, J. C. 1987. Estudio petrológico del granito de Villavieja de Yeltes (Salamanca). *Memória do Museu e Laboratório Mineralógico e Geológico da Faculdade de Ciências do Porto* **1**, 21–37.

Carracedo, M., Ortega Cuesta, L. A., Gil Ibarguchi, J. I. & Sánchez-Carretero, R. 1989. Aportación a la geoquímica de Tierras Raras (REE) en el batolito de Los Pedroches (Córdoba-España). *Stvdia Geologica Salmanticensia Volumen especial* **4**, 93–104.

Castro, A., Patiño Douce, A. E., Corretgé, L. G., de la Rosa, J. D., El-Biad, M. & El-Hmidi, H. 1999. Origin of peraluminous granites and granodiorites, Iberian massif, Spain. An experimental test of granite petrogenesis. *Contributions to Mineralogy and Petrology* **135**, 255–76.

Castro, A., Corretgé, L. G., El-Biad, M., El-Hmidi, H., Fernández, C. & Patiño-Douce, A. E. 2000. Experimental constraints on Hercynian anatexis in the Iberian massif, Spain. *Journal of Petrology* **41** (10), 1471–88.

Chappell, B. W. & White, A. J. R. 2001. Two contrasting granite types: 25 years later. *Australian Journal of Earth Sciences* **48**, 489–99.

Clarke, D. B. 1995. Cordierite in Felsic Igneous Rocks – a Synthesis. *Mineralogical Magazine* **59**, 311–25.

Clarke, D. B., Henry, A. S. & White, M. A. 1998. Exploding xenoliths and the absence of 'elephants' graveyards' in granite batholiths. *Journal of Structural Geology* **20**, 1325–43.

Clemens, J. D. & Vielzeuf, D. 1987. Constraints on melting and magma production in the crust. *Earth and Planetary Science Letters* **86**, 287–306.

Cook, P. J. 1992. Phosphogenesis around the Proterozoic–Phanerozoic transition. *Journal of the Geological Society* **149**, 615–20.

Cook, P. J. & Shergold, J. H. 1986. Proterozoic and Cambrian phosphorites – nature and origins. *In* Cook, P. J. & Shergold, J. H. (eds) *Phosphate deposits of the world*, 369–86. Cambridge: Cambridge University Press.

Davidson, L. R. & Mathison, C. I. 1974. Aluminous orthopyroxenes and associated cordierites, garnets and biotites from granulites of the Quairading district, Western Australia. *Neues Jahrbuch für Mineralogie Monatshefte* **6**, 272–87.

DePaolo, D. J. 1981. Trace element and isotopic effects of combined wall rock assimilation and fractional crystallization. *Earth and Planetary Science Letters* **53**, 189–202.

Díez Balda, M. A., Vegas, R. & González-Lodeiro, F. 1990. Autochthonous sequences in the Central Iberian Zone: Structure. *In* Dallmeyer R. D. & Martínez García, E. (eds) *Pre-Mesozoic geology of Iberia*, 172–88. Berlin: Springer.

Donaire, T., Pascual, E., Pin, C. & Duthou, J. L. 1999. Two-stage granitoid-forming event from an isotopically homogeneous crustal source: The Los Pedroches batholith, Iberian Massif, Spain. *Geological Society of America Bulletin* **111**, 1897–906.

Droop, G. T. R., Clemens, J. D. & Dalrymple, D. J. 2003. Processes and conditions during contact anatexis, melt escape and restite formation: the Huntly Gabbro Complex, NE Scotland. *Journal of Petrology* **44**, 995–1029.

Escuder Viruete, J., Indares, A. & Arenas, R. 2000. P–T paths derived from garnet growth zoning in an extensional setting: an example from the Tormes Gneiss Dome (Iberian Massif, Spain). *Journal of Petrology* **41**, 1489–515.

Evans, N. H. & Speer, J. A. 1984. Low-pressure metamorphism and anatexis of Carolina slate belt phyllites in the contact aureole of the Lilesville Pluton, North Carolina, USA. *Contributions to Mineralogy and Petrology* **87**, 297–309.

Fediuk, F. 1971. Cordierite in the Moldanubian gneisses. *Krystalinikum* **7**, 183–202.

Fernández, J., Hernández, A., Olivé, A., Carreras, F. J. & Capote, R. 1982. *Mapa geológico de España, E. 1:50000. Hoja 505 y Memoria*. Madrid: Instituto Geológico y Minero de España.

Finger, F. & Clemens, J. D. 1995. Migmatization and 'secondary' granitic magmas: effects of emplacement and crystallization of 'primary' granitoids in Southern Bohemia, Austria. *Contributions to Mineralogy and Petrology* **120**, 311–26.

Franco, M. P. & García de Figuerola, L. C. 1986. Las rocas básicas y ultrabásicas en el extremo Occidental de la Sierra de Avila (Provincias de Avila y Salamanca). *Stvdia Geologica Salmanticensia* **23**, 193–219.

Franco, M. P. & Sánchez, T. 1987. Características petrológicas del área de El Mirón (N del Valle del Corneja, provincia de Avila). *In* Bea, F., Carnicero, A., Gonzalo, J. C., López-Plaza, M. & Rodríguez Alonso, M. D. (eds) *Geología de los granitoides y rocas asociadas del Macizo Hespérico*, 293–314. Madrid: Rueda.

Furlong, K. P. & Myers, J. D. 1985. Thermal-mechanical modeling of the role of thermal stresses and stoping in magma contamination. *Journal of Volcanology and Geothermal Research* **24**, 179–91.

Gabaldón Lopez, V., Urroz, J. H., Lorenzo Alvarez, S., Picart Boira, J., Casanovas, J. S. & Pont, F. J. S. 1989. Sedimentary facies and stratigraphy of Precambrian–Cambrian phosphorites on the Valdelacasa anticline, Central Iberian Zone, Spain. *In* Notholt, A. J. G., Sheldon, R. P. & Davidson, D. F. (eds) *Phosphate deposits of the World, Volume 2: Phosphate rock resources*, 422–8. Cambridge: Cambridge University Press.

Gama Pereira, L. C. 1984. Sobre a ocorrência de fosfatos no granito de Pedrógão Grande (Portugal Central). *Publicações do Museu e Laboratório Mineralógico e Geológico da Universidade de Coimbra* **98**, 125–31.

García de Figuerola, L. C. & Franco, M. P. 1975. Las formaciones infraordovícicas y el borde de las granodioritas al E de Guijuelo (Salamanca). *Estudios Geológicos* **21**, 487–500.

García de Figuerola, L. C., Rodríguez Alonso, M. D., Bascones, L. & Martín, D. 1988. *Mapa geológico de España, E. 1:50000. Hoja 573 y Memoria*. Madrid: Instituto Geológico y Minero de España.

García Moreno, O., Corretgé, L. G. & Castro, A. 2007. Processes of assimilation in the genesis of cordierite leucomonzogranites from the Iberian massif: A short review. *Canadian Mineralogist* **45**, 71–85.

Gil Ibarguchi, J. I. & Martínez, F. J. 1982. Petrology of garnet–cordierite–sillimanite gneisses from the El Tormes thermal dome, Iberian Hercynian foldbelt (NW Spain). *Contributions to Mineralogy and Petrology* **80**, 14–24.

Glazner, A. F. 2007. Thermal limitations on incorporation of wall rock into magma. *Geology* **35**, 319–22.

Gordillo, C. E. 1979. Observaciones sobre la petrología de las rocas cordieríticas de la Sierra de Córdoba. *Boletín de la Academia Nacional de Ciencias, Córdoba, Argentina* **53**, 3–44.

Green, N. L. 1994. Mechanism for middle to upper crustal contamination: Evidence from continental-margin magmas. *Geology* **22**, 231–4.

Gribble, C. D. 1968. The cordierite-bearing rocks of the Haddo House and Arnage Districts, Aberdeenshire. *Contributions to Mineralogy and Petrology* **17**, 315–30.

Grove, T. L., Kinzler, R. J., Baker, M. B., Donnelly-Nolan, J. M. & Lesher, C. E. 1988. Assimilation of granite by basaltic magmas at Burnt Lava flow, Medicine Lake volcano, northern California: Decoupling of heat and mass transfer. *Contributions to Mineralogy and Petrology* **98**, 455–89.

Halliday, A. N., Stephens, W. E. & Harmon, R. S. 1981. Isotopic and chemical constraints on the development of peraluminous Caledonian and Acadian granites. *Canadian Mineralogist* **19**, 205–16.

Harrison, T. M. & Watson, E. B. 1984. The behaviour of apatite during crustal anatexis: equilibrium and kinetic considerations. *Geochimica et Cosmochimica Acta* **48**, 1467–77.

Healy, B., Collins, W. J. & Richards, S. W. 2004. A hybrid origin for Lachlan S-type granites: the Murrumbidgee Batholith example. *Lithos* **78**, 197–216.

Hernández, A., Fernández, J., Carreras, F. J. & Olivé, A. 1982. *Mapa geológico de España, E. 1:50000. Hoja 506 y Memoria*. Madrid: Instituto Geológico y Minero de España.

Hildreth, W. & Moorbath, S. R. 1988. Crustal contributions to arc magmatism in the Andes of central Chile. *Contributions to Mineralogy and Petrology* **98**, 455–89.

Ilyin, A. V. 1998. Rare-earth geochemistry of 'old' phosphorites and probability of syngenetic precipitation and accumulation of phosphate. *Chemical Geology* **144**, 243–56.

Jamieson, R. A. 1984. Low-pressure cordierite-bearing migmatites from Kelly's Mountain, Nova Scotia. *Contributions to Mineralogy and Petrology* **86**, 309–20.

Jung, S., Hoernes, S. & Mezger, K. 2000. Geochronology and petrogenesis of Pan-African, syn-tectonic, S-type and post-tectonic A-type granite (Namibia): products of melting of crustal sources, fractional crystallization and wall rock entrainment. *Lithos* **50**, 259–87.

Knesel, J. M., Davidson, J. P. & Duffield, W. A. 1999. Evolution of silicic magma though assimilation and subsequent recharge: Evidence from Sr isotopes in sanidine phenocrysts. *Journal of Petrology* **40**, 773–86.

Lev, S. M., McLennan, S. M. & Hanson, G. N. 1999. Mineralogic control on REE mobility during black-shale diagenesis. *Journal of Sedimentary Research* **69**, 1071–82.

López-Plaza, M. & Carnicero, A. 1987. El plutonismo Hercínico de la penillanura Salmantino-Zamorana (centro-oeste español). *In* Bea, F., Carnicero, A., Gonzalo, J. C., López-Plaza, M. & Rodríguez Alonso, M. D. (eds) *Geología de los granitoides y rocas asociadas del Macizo Hespérico*, 53–68. Madrid: Rueda.

Martín, D., Ugidos, J. M., Nozal, F. & Pardo, M. V. 1990. *Mapa geológico de España, E. 1:50000. Hoja 527 y Memoria*. Madrid: Instituto Tecnológico Geominero de España.

McArthur, J. M. 1980. Postdepositional alteration of the carbonate-fluorapatite phase of Moroccan phosphate. *In* Bentor, Y. K. K. (ed.) *Marine phosphorites*, 53–60. Tulsa: Society of Economic of Paleontologists and Mineralogists.

Miller, C. F. 1985. Are strongly peraluminous magmas derived from pelitic sedimentary sources? *Journal of Geology* **93**, 673–89.

Montel, J. M. & Vielzeuf, D. 1997. Partial melting of metagreywackes. Part II. Compositions of minerals and melts. *Contributions to Mineralogy and Petrology* **128**, 176–96.

Moreno-Ventas, I., Rogers, G. & Castro, A. 1995. The role of hybridization in the genesis of Hercynian granitoids in the Gredos Massif, Spain: inferences from Sr–Nd isotopes. *Contributions to Mineralogy and Petrology* **120**, 137–49.

Nell, J. 1985. The Bushveld metamorphic aureole in the Potgietersrus area: evidence for a two-stage metamorphic event. *Economic Geology* **80**, 1129–52.

Oczlon, M. S. & Díez Balda, M. A. 1992. Contourites in laminated black shale facies of the Aldeatejada Formation (Precambrian/Cambrian boundary range, province of Salamanca, western Spain). *Revista de la Sociedad Geológica de España* **5**, 167–76.

Odriozola, J. M., Peón, A., Ugidos, J. M., Pedraza, J. & Fernández, P. 1981a. *Mapa geológico de España, E. 1:50000. Hoja 577 y Memoria*. Madrid: Instituto Geológico y Minero de España.

Odriozola, J. M., Peón, A., Ugidos, J. M., Pedraza, J. & Fernández, P. 1981b. *Mapa geológico de España, E. 1:50000. Hoja 578 y Memoria*. Madrid: Instituto Geológico y Minero de España.

Patiño-Douce, A. E. 1999. What do experiments tell us about the relative contributions of crust and mantle to the origin of granitic magmas? *In* Castro, A., Fernandez, C. & Vigneresse, J.-L. (eds) *Understanding granites: Integrating new and classical techniques*, 55–75. London: The Geological Society.

Patiño-Douce, A. E. & Johnston, A. D. 1991. Phase equilibria and melt productivity in the pelitic system: implications for the origin of peraluminous granitoids and aluminous granulites. *Contributions to Mineralogy and Petrology* **107**, 202–18.

Perconig, E., Vázquez, F., Velando, F. & Leyva, F. 1986. Proterozoic and Cambrian phosphorite deposits: Fontanarejo, Spain. *In* Cook, P. J. & Shergold, J. H. (eds) *Phosphate deposits of the world, Volume 1: Proterozoic and Cambrian phosphates*, 220–34. Cambridge: Cambridge University Press.

Pitcher, W. S. 1997. *The Nature and Origin of Granite*. Glasgow: Chapman & Hall.

Rapela, C. W., Baldo, E. G., Pankhurst, R. J. & Saavedra, J. 2002. Cordieritite and leocogranite formation during emplacement of highly peraluminous magma: the El Pilón granite Complex (Sierras Panpeanas, Argentina). *Journal of Petrology* **43**, 1003–28.

Rasmussen, B., Buick, R. & Taylor, W. R. 1998. Removal of oceanic REE by authigenic precipitation of phosphatic minerals. *Earth and Planetary Science Letters* **164**, 135–49.

Recio, C., Fallick, A. E. & Ugidos, J. M. 1992. A stable isotopic ($\delta^{18}O$, $\delta D$) study of the late Hercynian granites and their host-rocks in the Central Iberian Massif (CIM, Spain). *Transactions of the Royal Society of Edinburgh: Earth Sciences* **83**, 247–57.

Riesco, M., Stüwe, K., Reche, J. & Martínez, F. J. 2004. Silica depleted melting of pelites. Petrogenetic grid and application to the Susqueda Aureole, Spain. *Journal of Metamorphic Geology* **22**, 475–94.

Rodríguez Alonso, M. D., Peinado, M., López-Plaza, M., Franco, P., Carnicero, A. & Gonzalo, J. C. 2004. Neoproterozoic–Cambrian synsedimentary magmatism in the Central Iberian Zone (Spain): geology, petrology and geodynamic significance. *International Journal of Earth Sciences* **93**, 897–920.

Saito, S., Arima, M. & Nakajima, T. 2007. Hybridisation of a shallow 'I-type' granitoid pluton and its host migmatite by magma-chamber wall collapse: the Tokuwa pluton, central Japan. *Journal of Petrology* **48**, 79–111.

Schreyer, W., Gordillo, C. E. & Werding, G. 1979. A new sodian-beryllian cordierite from Soto, Argentina, and the relationship between distortion index, Be content, and state of hydration. *Contributions to Mineralogy and Petrology* **70**, 421–8.

Smith, D. G. W. 1965. The chemistry and mineralogy of some emery-like rocks from Sithean, Sluaigh, Strachur, Argyllshire. *American Mineralogist* **50**, 1982–2022.

Spera, F. J. & Bohrson, W. A. 2001. Energy-constrained open system magmatic processes I: General model and energy-constrained assimilation and fractional crystallisation (EC–AFC) formulation. *Journal of Petrology* **42**, 999–1018.

Stevens, G., Clemens, J. D. & Droop, G. T. R. 1997. Melt production during granulite-facies anatexis: experimental data from 'primitive' metasedimentary protoliths. *Contributions to Mineralogy and Petrology* **128**, 352–70.

Taylor, S. R. & McLennan, S. M. 1985. *The continental crust: its composition and evolution*. London: Blackwell.

Ugidos, J. M. 1987. Características del metamorfismo de baja presión en zonas centro-occidentales españolas y su significado en relación con minerales alumínicos en los granitos. *Actas e Comunicaçoes de la IX Reunião sobre a Geologia do Oeste Peninsular, Porto, Portugal* **1**, 383–98.

Ugidos, J. M. 1988. New aspects and considerations on the assimilation of cordierite-bearing rocks. *Revista de la Sociedad Geológica de España* **1**, 129–33.

Ugidos, J. M. 1990. Granites as a paradigm of genetic processes of granitic rocks: I-types vs. S-types. *In* Dallmayer, R. D. & Martínez García, E. (eds) *Pre-Mesozoic Geology of Iberia*, 189–206. Berlin: Springer.

Ugidos, J. M., Rodríguez-Alonso, M. D., Martín, D. & Bascones, L. 1988. *Mapa geológico de España, E. 1:50000. Hoja 575 y Memoria*. Madrid: Instituto Tecnológico y Minero de España.

Ugidos, J. M., Rodríguez-Alonso, M. D., Colomer, A. & Martín, D. 1990. *Mapa geológico de España, E. 1:50000. Hoja 552 y Memoria*. Madrid: Instituto Tecnológico y Minero de España.

Ugidos, J. M., Armenteros, I., Barba, P., Valladares, M. I. & Colmenero, J. R. 1997a. Geochemistry and petrology of recycled orogen-derived sediments: a case study from Upper Precambrian siliciclastic rocks of the Central Iberian Zone, Iberian Massif, Spain. *Precambrian Research* **84**, 163–80.

Ugidos, J. M., Valladares, M. I., Recio, C., Rogers, G., Fallick, A. E. & Stephens, W. E. 1997b. Provenance of Upper Precambrian/Lower Cambrian shales in the Central Iberian Zone, Spain: evidence from a chemical and isotopic study. *Chemical Geology* **136**, 55–70.

Ugidos, J. M., Billström, K., Valladares, M. I. & Barba, P. 2003a. Geochemistry of the Upper Neoproterozoic and Lower Cambrian siliciclastic rocks and U–Pb dating on detrital zircons in the Central Iberian Zone, Spain. *International Journal of Earth Sciences* **92**, 661–76.

Ugidos, J. M., Valladares, M. I., Barba, P. & Ellam, R. M. 2003b. The Upper Neoproterozoic–Lower Cambrian of the Central Iberian Zone, Spain: Chemical and isotopic (Sm–Nd) evidence that the sedimentary succession records an inverted stratigraphy of its source. *Geochimica et Cosmochimica Acta* **67**, 2615–29. [Erratum: *Geochimica et Cosmochimica Acta* **68**, supplementary content, p. 1953.]

Ugidos, J. M. & Recio, C. 1993. Origin of cordierite-bearing granites by assimilation in the Central Iberian Massif (CIM, Spain). *Chemical Geology* **103**, 27–43.

Valladares, M. I., Ugidos, J. M. & Recio, C. 1993. Precámbrico Superior–Cámbrico Inferior en la Zona Centro-Ibérica: posible área fuente y criterios geoquímicos de correlación. *Revista de la Sociedad Geológica de España* **6**, 37–45.

Valladares, M. I., Barba, P., Colmenero, J. R., Armenteros, I, & Ugidos, J. M. 1998. La sucesión sedimentaria del Precámbrico superior–Cámbrico inferior en el sector central de la Zona Centro Ibérica: Litoestratigrafía, geoquímica y facies sedimentarias. *Revista de la Sociedad Geológica de España* **11**, 271–83.

Valladares, M. I., Barba, P., Ugidos, J. M., Colmenero, J. R. & Armenteros, I. 2000. Upper Neoproterozoic–Lower Cambrian sedimentary successions in the Central Iberian Zone (Spain): Sequence stratigraphy, petrology and chemostratigraphy. Implications for other European zones. *International Journal of Earth Sciences* **89**, 2–20.

Valladares, M. I., Barba, P. & Ugidos, J. M. 2002a. Precambrian. *In* Gibbons, W. & Moreno, T. (eds) *The Geology of Spain*, 7–16. London: The Geological Society.

Valladares, M. I., Ugidos, J. M., Barba, P. & Colmenero, J. R. 2002b. Contrasting geochemical features of the Central Iberian Zone shales (Iberian Massif, Spain): Implications for the evolution of Neoproterozoic–Lower Cambrian sediments and their sources in other Peri-Gondwanan areas. *Tectonophysics* **352**, 121–32.

Valladares, M. I., Ugidos, J. M., Barba, P., Fallick, A. E. & Ellam, R. M. 2006. Oxygen, carbon and strontium isotope records of Ediacaran carbonates in Central Iberia (Spain). *Precambrian Research* **147**, 354–65.

Valle Aguado, B., Azevedo, M. R., Schaltegger, U., Martínez Catalán, J. R. & Nolan, J. 2005. U–Pb zircon and monazite geochronology of Variscan magmatism related to syn-convergence extension in Central Northern Portugal. *Lithos* **82**, 169–84.

Villaseca, C., Barbero, L. & Rogers, G. 1998. Crustal origin of Hercynian peraluminous granitic batholiths of Central Spain: petrological, geochemical and isotopic (Sr, Nd) constraints. *Lithos* **43**, 55–79.

Watson, E. B. & Harrison, T. M. 1983. Zircon saturation revisited: temperature and composition effects in a variety of crustal magma types. *Earth and Planetary Science Letters* **64**, 295–304.

Zeck, H. P., Wingate, M. T. D. & Pooley, G. 2007. Ion microprobe U–Pb zircon geochronology of a late tectonic granitic–gabbroic rock complex within the Hercynian Iberian belt. *Geological Magazine* **144**, 157–77.

Zen, E. 1988. Phase-relations of peraluminous granitic-rocks and their petrogenetic implications. *Annual Review of Earth and Planetary Sciences* **16**, 21–51.

MS received 28 October 2008. Accepted for publication 8 June 2009.